M 2025

U.PORTO
FEUP FACULDADE DE ENGENHARIA
UNIVERSIDADE DO PORTO

ENHANCING THE STRUCTURAL INTEGRITY OF ALUMINIUM COMBINATION LADDERS: THE ROLE OF HEAT TREATMENT OPTIMISATION AND PRODUCTION PROCESS

ANA CATARINA MOREIRA FIGUEIREDO
MASTER'S DEGREE DISSERTATION IN MATERIALS ENGINEERING SUBMITTED TO THE FACULTY OF ENGINEERING OF UNIVERSITY OF PORTO

SUPERVISOR
PROFESSOR ELSA WELLENKAMP DE SEQUEIROS

CANDIDATO	Ana Catarina Moreira Figueiredo		Código 202005630
TÍTULO	Enhancing the Structural Integrity of Aluminium Combination Ladders: the Role of Heat Treatment Optimisation and Production Process		
DATA	11 de setembro de 2025		
LOCAL	Faculdade de Engenharia da Universidade do Porto – Sala F106 - 10:15		

JÚRI	*Presidente*	Laura Maria Melo Ribeiro	DEMec/FEUP
	Arguente	Fernando Jorge Lino Alves	DEMec/FEUP
	Orientador	Elsa Wellenkamp de Sequeiros	DEMec/FEUP

ABSTRACT

This dissertation was developed in cooperation between Ferral – José Luís & Ca. Lda. and the Faculty of Engineering of the University of Porto. This collaboration was motivated by the need to optimise the aluminium alloy selection process and enhance the mechanical properties of combination ladders, all with a focus on continuous improvement. The main goals of this project were to select the appropriate aluminium alloy and its heat treatment conditions to get a ladder approved for professional use. The work also aimed to improve the control and inspection process for raw materials, ultimately reducing the number of nonconforming products and the scrap rate.

The 6060 and 6061 alloys profiles were initially analysed in their as-received condition. The subsequent study focused on the 6060 alloy, where samples were solution heat treated at 520 ºC for 2 hours, followed by conventional ageing at 175 ºC or dual ageing treatment with final ageing temperatures of 185 ºC and 195 ºC and total ageing times of 4.5 and 6 hours. The samples were characterised using optical microscopy (OM), scanning electron microscopy with energy-dispersive spectroscopy (SEM/EDS) and hardness tests. Tensile tests were also carried out for the as-received samples. In addition, the production process of the ladders was analysed through three different zones corresponding to distinct processing stages, using Vickers hardness tests, and through computerised tomography analysis of the failure mechanism. To evaluate the mechanical performance under different conditions, strength tests were performed on ladders produced with 58 mm and 60 mm profiles.

In the as-received condition, the 6061 alloy demonstrated higher hardness and strength values compared to the 6060 alloy. The highest hardness for the 6060 alloy (92 HV10) was achieved through two conditions: conventional ageing at 175 ºC for 12 hours and dual ageing at 195 ºC for a total time of 6 hours. Microstructural analysis confirmed the presence of precipitates containing aluminium, iron, manganese and silicon, which were formed during solidification and solution heat treatment. This analysis also revealed slight differences in grain and precipitate sizes between samples. The production process analysis conclude that it has no significant influence on the ladder's failure mechanism. Finally, the ladder's strength tests led to the conclusion that the peak strength condition of the 6060 alloy is insufficient to achieve approval in the test, and that the 60 mm profiles showed better performance under the same conditions. The 6061 alloy, in the 58 mm profile, exhibited a positive response, successfully passing the test. However, the 60 mm profile presented dimensional nonconformities, which resulted in failure during the same test.

This study also concluded that strict control and inspection of raw material are crucial for reducing nonconformities and lowering the scrap rate, especially by monitoring the chemical composition, the profile wall thickness and its hardness value.

Keywords: Aluminium; 6060; 6061; Ageing Treatment; Precipitates; Strength; Ladders.

RESUMO

A presente dissertação foi desenvolvida em cooperação entre a Ferral – José Luís & Ca. Lda. e a Faculdade de Engenharia da Universidade do Porto. A motivação para esta parceria adveio da necessidade de otimização do processo de seleção de ligas de alumínio para a produção de escadas combinadas, assim como de otimização das suas propriedades mecânicas, numa constante visão de melhoria contínua. Os principais objetivos deste trabalho envolveram a seleção de ligas de alumínio e das suas condições de tratamento térmico para aprovação de uma escada para uso profissional e melhoria dos processos de controlo e inspeção da matéria-prima, de modo a diminuir o número de produtos não conformes e a consequente taxa de sucata.

As ligas 6060 e 6061 foram analisadas, na forma de perfis, tendo sido ambas caracterizadas na sua condição as-received. O seguimento do estudo focou-se na liga 6060, onde as amostras foram solubilizadas a 520 ºC durante 2 horas, seguido de envelhecimentos convencionais a 175 ºC ou envelhecimentos duplos com temperaturas finais de envelhecimento de 185 e 195 ºC e tempos totais de 4,5 e 6 horas. A caracterização das amostras envolveu microscopia ótica (MO), microscopia eletrónica de varrimento com espetroscopia de energia dispersiva (SEM/EDS), ensaios de durezas e, ainda, ensaios de tração no caso das amostras as-received. O processo de produção das escadas foi analisado, através de três zonas correspondentes a etapas do processo, recorrendo a ensaios de dureza Vickers, e através do mecanismo de falha, utilizando tomografia computorizada (CT). Para avaliar o desempenho mecânico das diferentes condições, foram realizados ensaio de resistências nas escadas, produzidas com perfis de 58 e 60 mm. Nas amostras as-received, a liga 6061 apresentou valores de dureza e resistência superiores às da liga 6060. Na liga 6060, as condições que permitiram a maximização da dureza (92 HV10) foram envelhecimento convencional a 175 ºC durante 12 horas e envelhecimento duplo a 195 ºC e tempo total de 6 horas. A análise microestrutural permitiu verificar a presença de precipitados formados durante a solidificação e solubilização, contendo alumínio, ferro, manganês e silício, assim como identificar ligeiras diferenças no tamanho de grão e de precipitados das diferentes amostras. A análise do processo de produção permitiu concluir que o mesmo não tem influência na falha do produto. Por último, os ensaios de resistência das escadas levaram à conclusão de que a condição de máxima resistência da liga 6060 não é suficiente para alcançar a aprovação no ensaio e que os perfis de 60 mm apresentam uma melhor resposta no mesmo. A liga 6061 no perfil de 58 mm apresentou uma resposta positiva ao ensaio, alcançando a aprovação, mas, no entanto, o perfil de 60 mm falhou o teste devido a não conformidades nas suas dimensões. Este estudo permitiu ainda concluir que um apertado controlo e inspeção da matéria-prima é fundamental para a redução de não conformidades e da taxa de sucata, fundamentalmente controlando a composição química, a espessura da parede do perfil e o seu valor de dureza.

Palavras-chave: Alumínio; 6060; 6061; Envelhecimento; Precipitados; Resistência; Escadas.

ACKNOWLEDGEMENTS

Firstly, I would like to express my gratitude to Prof. Elsa Sequeiros for the opportunity to be a part of this project and to develop myself, making me a more capable student and person. For all the guidance and support through this work, for all the transmitted knowledge, for always trying to add something new and better to this dissertation and for always trusting me.

To Prof. Manuel Vieira, I am extremely grateful for always be willing to collaborate with this dissertation and to assist in its development.

To Ing. Bernardo Ribeiro, I am very thankful for all the help, motivation and friendship during this dissertation, and for the full availability to answer my questions.

I would also like to address my gratitude to all the teachers of the Materials Engineering degree of the Faculty of Engineering of University of Porto (FEUP), for all the imparted knowledge and for all the availability to always answer to my questions or to help solve my problems. I would like to thank to Prof. Laura Ribeiro, Prof. Ruben Santos and Prof. Luís Filipe Malheiros, who profoundly influenced me by consistently emphasizing the value of professionalism allied with empathy.

I also would like to thank Sr. Ramiro, D. Cândida and D. Maria José, for always helping in the developing of this work and for always make sure that I had everything that I may needed.

To my friends and colleagues from FEUP who turned this experience a lot better, by always being there when needed and by supporting me. In a more special way, I would like to thank to Mariana Truta, Rui Marques, Regina, Mariana, Tiago, Rui Festas, Paulo and João, for all the moments we lived together in these five years and for never letting go of me.

Lastly, the most special and meaningful thanks to my family, who always believed in me, supported me and helped me in every way. To my parents for all the love, comprehension and support, allowing me to be the person I am today. To my sister, for all the patience, friendship and confidence. To João, for all the kindness, comfort, and everlasting understanding.

INSTITUTIONAL ACKNOWLEDGEMENTS

Firstly, I acknowledge Ferral – José Luís & Ca. Lda. for the opportunity to develop this work and for choosing me to be a part of it. To Dr. Luís Filipe, Ing. Pedro Maia, Marta and André for always being available to answer my questions and to help me through this process, for always making sure I had the necessary conditions and for all the transmitted knowledge.

I also acknowledge Mechanical Engineering Department and Faculty of Engineering of University of Porto for providing me with the necessary equipments and conditions.

INDEX

LIST OF FIGURES

LIST OF TABLES

LIST OF ABBREVIATIONS

AA	Aluminium Alloy(s)
Al	Aluminium
AES	Atomic Emission Spectroscopy
Cr	Chromium
CT	Computerised Tomography
Cu	Copper
DA	Dual Ageing
DE	Direct Extrusion
EDS	Energy-dispersive X-ray Spectroscopy
Fe	Iron
GP	Guinier-Preston
IE	Indirect Extrusion
Mg	Magnesium
Mn	Manganese
SEM	Scanning Electron Microscopy
SDG	Sustainable Development Goals
SHT	Solution Heat Treatment
Si	Silicon
TEM	Transmission Electron Microscopy
Zr	Zirconium

1. INTRODUCTION

This dissertation was carried out in cooperation between the Faculty of Engineering of the University of Porto (FEUP) and FERRAL - José Luís & CA. Lda., for the fulfilment of the master's degree in Materials Engineering. This first chapter provides a comprehensive overview of the dissertation's subject of analysis, outlining its main objectives and describing the organisation of this document.

1.1. FERRAL - José Luís & CA. Lda.

Ferral – José Luís & Ca. Lda. is a Portuguese company and a market leader in solutions for working at height, with over 40 years of experience. The company focuses on developing products that combine safety, lightness, ease of use, multifunctionality, and space efficiency. Its main product range includes stepladders, ladders, scaffolding, multi-purpose systems and platforms [1].

Ferral is certified under ISO 9001 and ISO 14001 standards, ensuring quality and environmental management. In addition, all products comply with the applicable European and international standards, including EN131-1, EN131-2, EN131-3, EN131-4, NF E85-200, EN14183, EN1004 and NF P93-352 [2].

Committed to continuously improving its products and processes, Ferral has been developing projects in collaboration with academic institutions, aiming to optimise them and ensure constant adaptation to market demands.

1.2. Contextualisation and Motivation

Aluminium ladders comprise a significant portion of the global ladder market, thanks to aluminium's inherent properties, such as its low density, high specific strength, corrosion resistance, and excellent recyclability [3]. This industry is driven not only by the inherent advantages of aluminium but also by the vast array of innovations and modifications made possible through the selection of different alloys with specific properties, as well as by optimising overall product design. Thus, the choice of the alloy and the definition of its processing route, particularly the heat treatment, are essential, as they directly influence the mechanical properties of the final product [4].

The development of this project, titled "Enhancing the Structural Integrity of Aluminium Combination Ladders: The Role of Heat Treatment Optimisation and Production Process" was predominantly driven by the necessity to achieve product approval for professional application in compliance with the EN131-2 standard. The opportunity to optimise aluminium alloy properties, either through heat treatment parameters modification or through enhancements in the internal manufacturing process of the ladder, constitutes a significant advantage for the organisation.

This approach enables improved economic efficiency and profitability, while concurrently minimising the amount of scrap produced during testing with various alloys, which are frequently carried out without comprehensive optimisation studies.

Therefore, a thorough and well-founded analysis of the most relevant alloys for this product was the primary motivation for conducting this work. The ultimate aim was to develop a product that is as optimised as possible, both in terms of performance and economic and commercial viability.

1.3. Objectives and Strategy

The development of this dissertation involved not only objectives related to the product itself, but also associated with the process of raw material control and inspection conducted by the company. Consequently, the primary objectives of this work can be delineated as follows:

- Implementation of a structured process for the control and inspection of raw materials.
- Compliance intervals establishment for the key properties of the profiles evaluated upon receipt of raw materials.
- Selection of the most appropriate alloy for manufacturing the studied product.
- Heat treatment parameters optimisation for enhancing the mechanical performance of the final product.
- Analysis and optimisation of the product's manufacturing process.
- Reduction of the production scrap rate.
- Maximum optimisation of the final product, in terms of performance and economic efficiency.

Throughout the dissertation, several sustainable development goals (SDG) were also considered, namely:

- Investing in more efficient manufacturing processes with lower energy consumption (SDG 7 - Affordable and clean energy; SDG 9 – Industry, Innovation and Infrastructure).
- Reducing material waste, thus promoting responsible consumption and production (SGD 12 – Responsible Consumption and Production).
- Implementing collection and treatment programmes for aluminium scrap, fostering circular economy practices and reducing environmental impact (SDG 13 – Climate Action).

Figure 1 illustrates the scheme of the strategy employed to achieve the objectives outlined earlier.

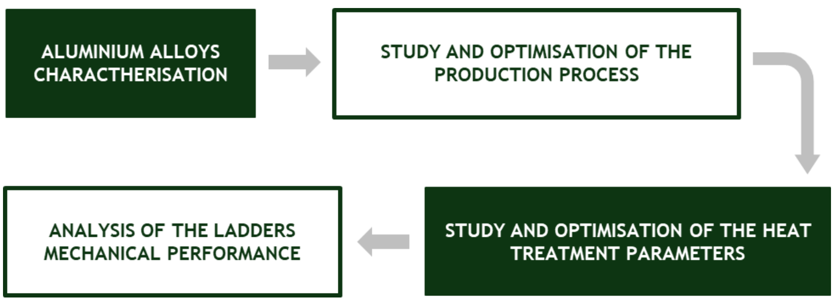

Figure 1: Scheme of the used strategy.

1.4. Dissertation Structure

This dissertation is organised into six chapters. Chapter 1, the present chapter, outlines the central research subject and the circumstances under which the research was conducted. It further articulates the context and motivation for the study, followed by the establishment of the objectives for this dissertation. In Chapter 2, a comprehensive literature review is offered, encompassing the theoretical fundamentals deemed essential for the practical progression of the research. Particular emphasis is placed on aluminium, its alloys, the production process and its parameters, including extrusion and heat treatments, as well as their impact on the ultimate mechanical properties of the product.

Chapter 3 delineates the materials and methods employed, providing a comprehensive account of the experimental procedures, including the equipment and consumables utilised. Chapter 4 presents the results and pertinent discussion, elucidating the hypotheses that underpin the findings obtained.

Finally, Chapters 5 and 6 present, respectively, the conclusions drawn from this study and the bibliographic references that underpinned and guided the research.

It is also worth noting that this dissertation led to the approval of the topic for presentation at the Doctoral Congress in Engineering 2025 (DCE), through the display of a poster and a short oral presentation. The poster from this conference is presented in Appendix A.

2. LITERATURE REVIEW

This chapter delineates the literature review's primary themes relevant to this study's subject. Essential information for a thorough comprehension of the document has been collected and analysed. The covered content encompasses the material under investigation, with particular emphasis on the characterisation of the alloy and its properties, the production process of the studied product and its parameters and the impact of these factors on the performance of the final product.

2.1. Aluminium

In recent years, aluminium (Al) has established itself as a material of increasing interest to the industry owing to its combination of properties that make it suitable for multiple applications. The most relevant properties are its low density (approximately 2.7 g/cm3), its high corrosion resistance, and its high specific strength and stiffness. The exceptional corrosion resistance occurs because, when exposed to air, a layer of Al oxide forms on the material's surface. Additionally, pure Al exhibits easy machinability and interesting electrical and thermal conductivity, all while being associated with a low price [5]. For this reason, Al alloys have been widely chosen for many industries, such as shipbuilding, mechanical manufacturing, construction and the automotive industry. Nowadays, steel is being progressively replaced by Al and other lightweight alloys in applications requiring medium to high strength, along with high corrosion resistance and weldability, but where the lightweight is a crucial property [6]. For this reason, Al represents the most used non-ferrous metal in the world. Based on this, the need for improved mechanical properties to better serve current applications or to allow its use in new and demanding applications is driving the continuous development of new aluminium alloys [7].

Focusing on one of the most essential properties of this material, nowadays, a larger fraction of recycled Al is used to produce new products; however, many products are still produced solely with primary Al [8]. To produce one tonne of primary Al, approximately 14,000 kWh of energy is required. On the other hand, to recycle one tonne of Al, only 5% of the energy required for producing virgin Al is needed, and there is no significant difference in the quality of the virgin and recycled Al alloys [5]. However, there is a challenge with this production method, which is the chemical composition of the recycled Al, as it is difficult to control the level of impurities and the final composition of the alloy due to the various sources of Al to be recycled [7].

The extensive application of Al across various industrial sectors is primarily due to its diverse alloys, which will be elaborated upon in the subsequent section, rather than the use of pure Al.

2.1.1. Aluminium Alloys and their classification

Aluminium alloys (AA) are usually divided into two major groups: casting AA and wrought AA. In the first case, the product's final shape is obtained through casting processes. In contrast, in the second case, the material undergoes mechanical processes to achieve its final shape or geometry [9,10].

Another approach to classify AA and subdivide the previous groups is to determine whether they can be strengthened by heat treatment, referred to as heat treatable or non-heat treatable alloys. Figure 2 presents the overall classification and the designation of each alloy system and series [10].

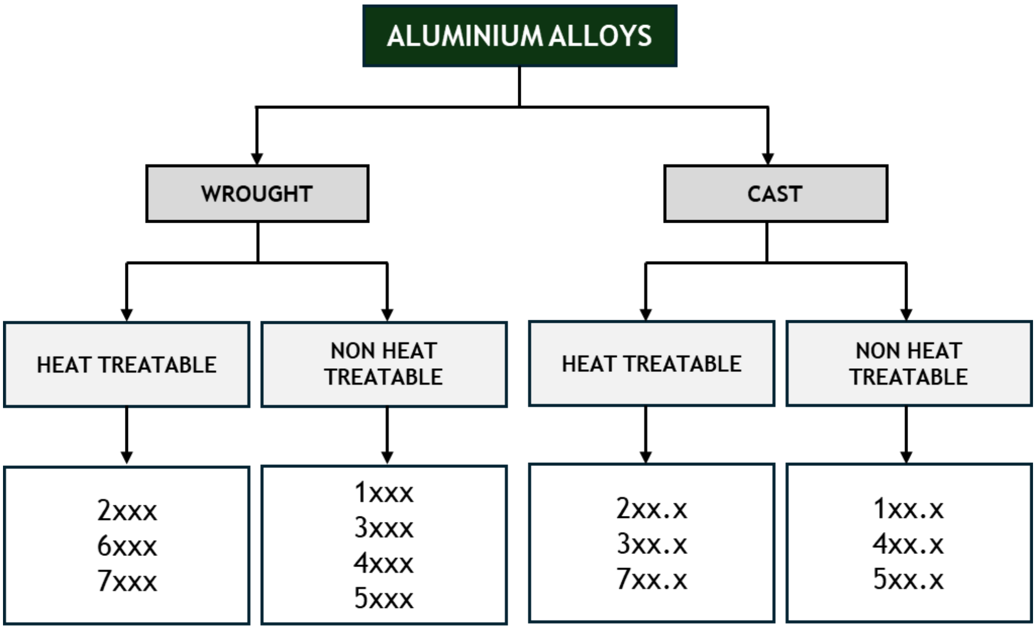

Figure 2: Classification of aluminium alloys [10].

This work will focus on the wrought AA, which will be further analysed in the following section.

2.1.2. Wrought Aluminium Alloys

Wrought AA are characterised by attaining their final form through mechanical processes, including extrusion, rolling, forging, and drawing. These procedures impart a controlled microstructure and a refined grain configuration, enhancing mechanical properties and enabling greater control over them. As previously noted, these alloys may also be categorised into two groups depending on their ability to be strengthened via heat treatment or not [9,11].

Furthermore, AA are systematically identified and classified according to a series number, determined by their primary alloying element. This classification utilises a four-digit system proposed by the Aluminium Association [11]. The relationship between each series and its corresponding main alloying element is illustrated in Table 1 [9].

Table 1: Main alloying element and properties of the aluminium alloys series [9].

SERIES	MAIN ALLOYING ELEMENT	PROPERTIES
1XXX	Aluminium content between 98.8 and 99.99 wt%	Excellent corrosion resistance, good electrical and thermal conductivity, good workability
2XXX	Copper (heat treatable)	High strength by solution heat treatment. Can be strengthened by solution heat treatment.
3XXX	Manganese (non-heat treatable)	Good workability combined with moderate strength.
4XXX	Silicon (non-heat treatable)	Sufficient quantities of silicon reduce the melting point of aluminium
5XXX	Magnesium (non-heat treatable)	HIgh strength, good weldability, good workability, and excellent corrosion resistance in marine environments and good weldabilty
6XXX	Magnesium and silicon (heat treatable)	High strength, good weldability, good workability and excellent corrosion resistance
7XXX	Zinc (heat treatable)	Very high strength and good fracture toughness
8XXX	Iron and Silicon	High strength and good formability
9XXX	Unused	High strength

2.1.3. Heat Treatable aluminium alloys

Certain AA respond favourably to heat treatment processes. These alloys can be strengthened through controlled heating and cooling cycles, employing two primary heat treatments: solution heat treatment (SHT) and ageing, via precipitation hardening. In such instances, the alloy's mechanical properties, notably its hardness and tensile strength, can be improved by precipitation of a secondary phase within the Al matrix. This process should be meticulously optimised to achieve the phase transformation that yields the maximum strength of the alloy. A more comprehensive analysis of the specific parameters of this process will be provided in section 2.2.2. The wrought AA that fall within this classification belong to the 2xxx, 6xxx, and 7xxx series. To facilitate precipitation hardening, two principal conditions must be satisfied: a substantial solubility of one component in the other, and a solubility limit that diminishes as temperature decreases [9]. Based on the processes applied to the alloy, there is a classification for heat treatments performed on aluminium alloys, which will be presented below.

2.1.4. Treatments Classification

Different heat and mechanical treatments can be applied to the alloys based on the desired microstructural characteristics and mechanical properties for the final application. Therefore, the designation of the treatment for each alloy is generally presented after its name, separated by a hyphen, and it includes a “T” followed by an algorism. When variations are applied to the primary treatment, an algorism may be added to the treatment designation [12].

The primary treatments for aluminium alloys are [12]:

T1 – The material is cooled from an elevated temperature shaping process, like casting or extrusion, and suffers natural ageing until it reaches a stable condition;

T2 – There is a cooling from an elevated temperature shaping process, like in T1, but after that, there is a cold-work step to improve its strength after cooling before the natural ageing process;

T3 – The material goes under a solution heat treatment and then it suffers a cold-work process, followed by a natural ageing process, like the two treatments above;

T4 – The first process is a solution heat treatment, to obtain a supersaturated solid solution, and after that, the material goes under a natural ageing process at room temperature;

T5 – An elevated temperature shaping process takes place, followed by an artificial ageing process;

T6 – In this treatment, a solution heat treatment is used to promote the maximum hardening through an artificial ageing process;

T7 – The same as the previous one, but there is an overaging of the material, to provide better results at some other properties that are not strength, like resistance to stress corrosion cracking or exfoliation corrosion;

T8 – Involves a solution heat treatment followed by a cold work process, which takes place before the artificial ageing one;

T9 – The same process as the T8 take place but in a different order. The solution heat treatment prepares the material for the artificial ageing process, and after precipitation hardening has occurred, the material undergoes a cold working process;

T10 – The processes used remain the same as in T3, but artificial ageing replaces natural ageing.

Each step of the treatments will be described in this chapter in Section 2.2, focusing on each parameter and its influence on the final properties of the alloy.

2.1.5. Al-Mg-Si systems – 6xxx series

6xxx AA system plays a vital role in engineering applications, being widely used in extrusion products due to its excellent malleability [9,10].

6xxx AA present up to 1.5 wt% of each magnesium (Mg) and silicon (Si), generally in a ratio that allows the formation of Mg_2Si. This series can also be split into three groups based on the wt% amount of magnesium and silicon in the alloy. In the first one, the wt% amount of Mg and Si does not exceed 1.5; these elements are in a balanced ratio condition or with a slightly higher silicon value. The most common alloy of this group is 6063 AA, which presents a Mg and Si amount of 1.1 wt% and is widely used in extrusion products. This alloy only requires a solution heat-treating temperature above 500 ºC, and it exhibits low quench sensitivity, which means that a separate SHT is unnecessary after the extrusion process. Consequently, it can be air quenched and then artificially aged to improve its strength. The second group includes alloys with a Mg and Si content higher than 1.5 wt% and a chemical composition that provides for additions of copper (Cu) up to 0.3 wt%, aiming to enhance the strength gain during heat treatment. Other elements, such as manganese (Mn), zirconium (Zr), and chromium (Cr), are also used to control the grain structure. These alloys usually achieve strengths about 70 MPa higher than those of the first group when a T6 treatment is applied. On the other hand, these alloys typically require a SHT temperature higher than that (530 to 560 ºC), followed by a quick quenching, and then artificial ageing treatment. The last group includes alloys with a significant excess of silicon, where adding 0.2 wt% Si to alloys with 0.8 wt% increases strength by about 70 MPa, while larger Si excesses are less effective. It is possible that Si segregation at grain boundaries occurs and can cause fracture after recrystallisation, but the addition of Mn, Cr, or Zr may prevent this. Some examples of this group's alloys are AA6351, AA6009 AND AA6262 [12].

In most industries, the Si content of 6060 AA is closest to the maximum value of its chemical composition range, since it forms, with Mg, the hardening precipitates. In contrast, the iron (Fe) and Cr contents are kept as close to the minimum range limit, since a higher content of these elements leads to the formation of brittle intermetallic compounds, which act as stress concentrators and degrade the ductility and toughness of the alloy [13]. Recently, the desire for the use of larger amounts of scrap material in the production processes is increasing, due to the implementation of new laws, which leads to higher contents of Fe and Cr in the alloy and may increase the possibility of forming AlFeSi particles, thereby reducing the alloy's workability [14].

The mechanical properties of 6060 AA containing a higher proportion of scrap material were comparable, exhibiting variations of less than 10%. To observe the Mg2Si particles, transmission electron microscopy (TEM) analysis may be required [14].

The advantages of Al-Mg-Si alloys, in comparison with other AA systems, include moderate strength (around 100 to 500 MPa), commendable toughness, exceptional corrosion resistance, favourable formability, enhanced weldability, and good machinability [10]. Specific values regarding the mechanical properties of some of these alloys will be provided later in this chapter on section 2.1.6.

To sum up, the 6xxx series of AA is extensively applied in extruded products and manufacturing processes owing to its superior workability. This characteristic, as with other mechanical properties, is highly dependent on the microstructural condition of the alloys. Approximately two-thirds of all extruded products are fabricated from Al, with roughly 90% of these originating from the 6XXX series [15].

2.1.6. 6060, 6063 and 6061 Aluminium Alloys

2.1.6.1. 6060 Aluminium Alloy

6060 AA is one of the most used 6xxx alloys, especially in the European market [16]. This alloy is commonly used to produce thin profiles, and those products are suitable for surface finishing, exhibiting an excellent response to painting and anodising. The chemical composition ranges of this alloy are presented in Table 2.

Table 2: Chemical composition ranges of the 6060 AA [17].

6060 AA: CHEMICAL COMPOSITION										
ELEMENT	**Al**	**Cr**	**Cu**	**Fe**	**Mg**	**Mn**	**Si**	**Ti**	**Zn**	**Other**
wt%	97.8 - 99.2	0 - 0.05	0 - 0.1	0.1 - 0.3	0.35 - 0.6	0 - 0.1	0.3 - 0.6	0 - 0.1	0 - 0.15	0 - 0.15

This alloy has a density value of 2690 to 2730 kg/m^3 and a price of 2.58 to 3.66 €/kg [17]. The most typical heat treatments applied to this alloy are T4 and T6. For both, the expected values for the most relevant mechanical properties are presented in Table 3.

Table 3: Mechanical properties ranges of the 6060 AA [17].

MECHANICAL PROPERTIES	T4		T6		
	MIN	MAX	MIN	MAX	
SPECIFIC STIFFNESS	25.7	27.1	25.6	27.9	MN.m/kg
YIELD STRENGHT	60	70	150	175	MPa
TENSILE STRENGHT	130	152	190	222	MPa
SPECIFIC STRENGHT	22.2	25.9	55.3	64.5	kN.m/kg
ELONGATION	15	21.6	8	11.5	%
COMPRESSIVE STRENGHT	60	70	150	175	MPa
FLEXURAL STRENGHT	60	70	150	175	MPa
POISSON'S RATIO	0.325	0.335	0.325	0.335	
HARDNESS - VICKERS	52	58	86	94	HV
HARDNESS - BRINNEL	48	53	81	89.2	HB
FATIGUE STRENGTH 10^7 CYCLES	56.4	65.8	68.4	79.8	MPa

Based on the EN 755-2:2016 standard, the minimum acceptable values for the tensile strength, yield strength, and elongation of a 6060 AA extruded profile are 190 MPa, 150 MPa, and 8%, respectively [16].

Menapace et al. (2021) studied the typical microstructure of 6060 AA after artificial ageing, indicating that, by scanning electron microscope (SEM) analysis, only the precipitates from solidification and SHT can be identified, as shown in Figure 3 [16]. For identification of the hardening precipitates, as the ß'' particles, TEM was used on the same study, resulting in Figure 4 [16].

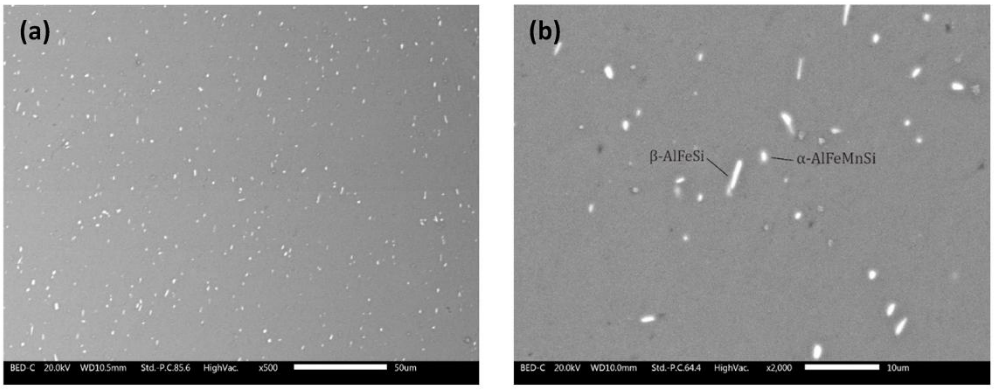

Figure 3: SEM images of the microstructure of the 6060 AA [16].

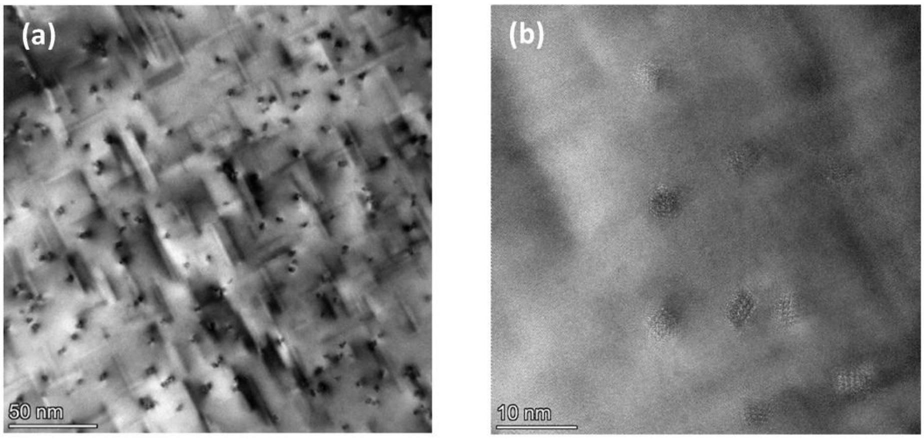

Figure 4: TEM images of the ß'' particles [16].

2.1.6.2. 6063 Aluminium Alloy

The 6063 AA is a structural alloy commonly used for extrusion products, such as window frames, stair rails, pipe rails and ladders. This alloy offers an excellent surface finish and improved extrudability compared to other Al-Mg-Si alloys, such as 6061, but on the other hand, it has lower strength. For that reason, 6063 is more commonly used in applications where better formability is required, such as complex extrusion products, and where a moderate strength is sufficient. Regarding the most important physical property, the density value of this alloy ranges from 2660 to 2720 kg/m^3, which is very similar to the density value of 6060 AA [18]. The chemical composition ranges of this alloy are presented in Table 4.

Table 4: Chemical composition ranges of the 6063 AA [18].

6063 AA: CHEMICAL COMPOSITION										
ELEMENT	Al	Cr	Cu	Fe	Mg	Mn	Si	Ti	Zn	Other
wt%	97.5 - 99.4	0 - 0.1	0 - 0.1	0 - 0.35	0.45 - 0.9	0 - 0.1	0.2 - 0.6	0 - 0.1	0 - 0.1	0 - 0.15

As done for the 6060 AA, the expected values for the most relevant mechanical properties of 6063 AA are presented in Table 5, for T4 and T6 treatments.

Table 5: Mechanical properties ranges of the 6063 AA [18].

MECHANICAL PROPERTIES	T4		T6		
	MIN	MAX	MIN	MAX	
SPECIFIC STIFFNESS	24.9	26.3	25.8	27.2	MN.m/kg
YIELD STRENGHT	70	81.6	205	225	MPa
TENSILE STRENGHT	130	152	215	241	MPa
SPECIFIC STRENGHT	26	30.3	76.1	83.8	kN.m/kg
ELONGATION	16	23	9	13	%
COMPRESSIVE STRENGHT	70	81,6	205	225	MPa
FLEXURAL STRENGHT	70	81.6	205	225	MPa
POISSON'S RATIO	0.325	0.335	0.325	0.335	
HARDNESS - VICKERS	48	53	76	84	HV
HARDNESS - BRINNEL	48	53	71	79	HB
FATIGUE STRENGTH 10^7 CYCLES	57.5	67	76.5	89.3	MPa

Nandy *et al.* [19] analysed the influence of ageing on the mechanical properties of the 6063 AA. The authors investigated the impact of ageing time variation on a T6 treatment with artificial ageing at 175 °C, ranging from 10 minutes to 14 days, by analysing the hardness and tensile properties of the alloy for each condition, developing a correlation between those two mechanical properties. The article concluded that, at the peak condition, the hardness value was 89 HV. This value is even slightly higher than the one presented (Table 5), suggesting that the alloy may achieve the desired range of mechanical properties. In another investigation, Munitz *et al.* [20] studied the ageing impact on the mechanical properties and microstructure of 6063 AA, also performing a T6 treatment, with a focus on the tensile properties. At the maximum strengthening condition, a tensile strength of 243 MPa was achieved, together with a yield strength of 216 MPa and an elongation of 8%. These values are consistent with the ones presented in Table 5, also confirming them. The typical microstructure of 6063 AA is very similar to the 6060 AA, shown in Figure 3.

2.1.6.3. 6061 Aluminium Alloy

6061 AA is commonly used in applications where a higher strength is required, such as in some aerospace applications, as it presents higher hardness and strength values compared to 6060 and 6063 AA [12]. The 6061 AA presents a higher concentration of alloying elements than the 6060 and 6063 alloys, with an excess of Mg, which increases the hardness and tensile strength but decreases the ductility and toughness [21]. The chemical composition ranges of this alloy are expressed in Table 6 [22].

Table 6: Chemical composition ranges of the 6061 AA [22].

6061 AA: CHEMICAL COMPOSITION										
ELEMENT	Al	Cr	Cu	Fe	Mg	Mn	Si	Ti	Zn	Other
wt%	95.8 - 98.6	0.04 - 0.35	0.15 - 0.4	0 - 0.7	0.8 - 1.2	0 - 0.15	0.4 - 0.8	0 - 0.15	0 - 0.25	0 - 0.15

The 6061 AA exhibits a density range of 2690 to 2730 kg/m^3 and, as mentioned earlier, this alloy can achieve higher hardness and strength due to its higher concentration of alloying elements, especially Cu [12]. The expected range of mechanical properties with T4 and T6 treatments is presented in Table 7.

Table 7: Mechanical properties ranges of the 6061 AA [22].

MECHANICAL PROPERTIES	T4		T6		
	MIN	MAX	MIN	MAX	
SPECIFIC STIFFNESS	24.5	25.8	24.5	25.8	MN.m/kg
YIELD STRENGHT	110	145	240	280	MPa
TENSILE STRENGHT	206	240	290	338	MPa
SPECIFIC STRENGHT	40.5	53.5	88.4	103	kN.m/kg
ELONGATION	16	23	10	14.4	%
COMPRESSIVE STRENGHT	110	145	240	280	MPa
FLEXURAL STRENGHT	110	145	240	280	MPa
POISSON’S RATIO	0.325	0.335	0.325	0.335	
HARDNESS - VICKERS	74	87	100	107	HV
HARDNESS - BRINNEL	62	68	90	100	HB
FATIGUE STRENGTH 10^7 CYCLES	91,1	106	112	131	MPa

Ozturk *et al.* [15] investigated the effect of ageing treatment on the mechanical properties of 6061 AA, employing various T6 treatments with different ageing durations at 200 ºC. At the condition where the maximum strengthening of the alloy was achieved, the hardness value was close to 95 HV, and the tensile properties were approximately 270 MPa, 320 MPa, and 13.2% for yield strength, ultimate strength, and elongation, respectively. These results align with those presented in Table 7. Additionally, Demir *et al.* [23] employed the same approach to investigate the effect of ageing on the machinability of 6061 AA, using an ageing temperature of 180 ºC. At the maximum strengthening condition, a hardness of 106 HV was achieved, a value that matches the range presented before. Figure 5 illustrates the typical microstructure of a 6061 AA after T6 treatment, obtained in a previous study [24].

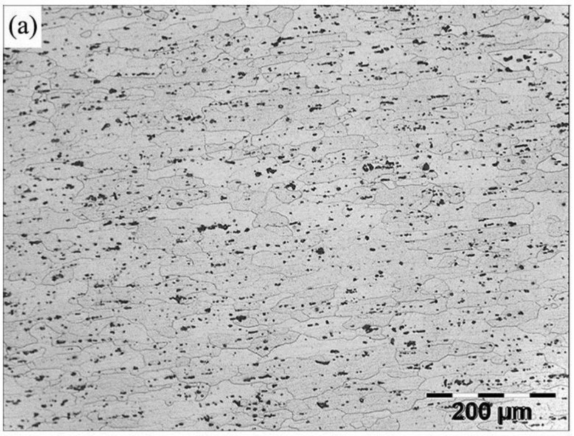

Figure 5: Microstructure of a 6061 AA [24].

2.2. Process

The process plays a significant role in the mechanical properties of the final product, as a variation or change in a parameter can cause a different mechanism to occur and completely alter the final properties of the AA. In this section (2.3), two processes will be discussed: extrusion and heat treatment, including each step of the latter.

2.2.1. Extrusion

Extrusion is a process in which a solid billet is deformed using a die and is pushed through to create a constant cross-sectional shape or profile, determined by the shape of the die [25].

Metal extrusion can be performed with or without the application of temperature, that is, as hot extrusion or cold extrusion. The hot extrusion process is typically used when a significant deformation of the billet is required to achieve a highly reduced cross-sectional area. This process is commonly used for non-ferrous materials, such as Al, due to its need for lower working temperatures, unlike steel [25,26,27].

On the other hand, room-temperature extrusion allows for better precision in the process, as the profile is not exposed to dimensional variations resulting from the applied temperature. Additionally, a cold extrusion process enables the achievement of a gain in strength during material deformation, as it is a cold work process.

Metal extrusion can be divided into two major distinct processes: direct or forward extrusion and indirect or backwards extrusion. There are, however, other types of extrusion, such as hydrostatic and impact extrusion.

2.2.1.1. Direct Extrusion

Direct extrusion (DE) can be characterised by a billet being forced through the die using a ram or a hydraulic press to force that movement. In another way, DE is the process where the direction of the metal flow is the same as the movement of the ram. This process is commonly used for non-ferrous material, especially in AA sections [25,28]. This process is easy to operate, and the used die is usually simple. An existing problem in this process is the higher friction that exists between the metal and the container walls when the ram forces the billet to slice toward the die, resulting in a significant increase in the ram force required for this process [27]. A scheme representing this process is presented in Figure 6.

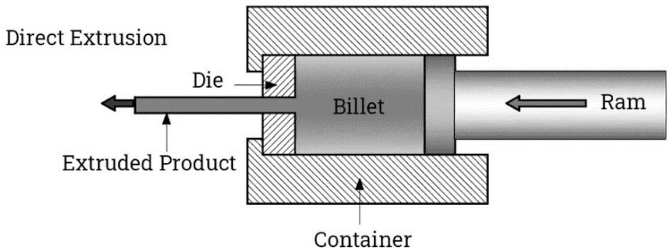

Figure 6: Scheme of the DE process [26].

2.2.1.2. Indirect Extrusion

On the other hand, in indirect extrusion (IE), a shaped ram is pushed into the billet, while the chamber holds the billet, and a dead zone is formed, as shown in Figure 7. In this process, the direction of the metal flow is opposite to that of the extrusion bearing. This process is typically used with materials that exhibit poor ductility [25,28]. There is no relative movement between the billet and the container, a factor that reduces the power required for the process, as there is no friction between the two parts [27,28].

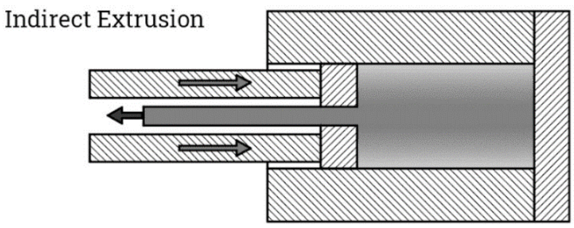

Figure 7: Scheme of the IE process [26].

2.2.1.3. Aluminium Extrusion: Parameters and their influence

The properties of the extruded product depend on several parameters, including extrusion ratio, extrusion speed, die type, and others. The most relevant parameters are [27]:

- **Type of extrusion process**: the relation between the direction of the metal flow and the ram flow, that is, whether DE or IE is used in the process, since the used process determines if there is friction or not, for example.
- **Die type and Design**: extrusion dies can be solid, semi-hollow or hollow dies, and the die design determines the conditions of the metal extrusion.
- **Types of Aluminium Alloys**: each AA requires different process parameters. The most widely used in extrusion are the 6xxx Series AA.
- **Extrusion Temperature**: this parameter influences how the metal is going to flow, but also influences the oxidation rate of the materials.
- **Extrusion ratio**: it presents the relationship between the billet and the die cross-sectional areas, as a larger ratio means a higher deformation, which requires a higher extrusion pressure.
- **Extrusion speed**: the speed at which the metal flows through the die, and a higher speed means a higher extrusion pressure needed and a higher exit temperature. For this reason, this parameter must be balanced to control the same factor.
- **Length of the billet:** this parameter influences the extrusion pressure and the extrusion ratio.

Given that, the Al extrusion must follow optimised parameters, which should be defined for each alloy.

Previous studies [29] mention that the optimal range of extrusion temperature for 6060 and 6063 AA is from 400 to 500 ºC, since this range allows the optimisation of the material's flow, decreasing the flow stress, and helps the dissolution of previously formed precipitates.

Chahare *et al*. [30] studied the optimisation of the Al extrusion process for 6063 AA using the Taguchi method, obtaining a billet pre-heating temperature of 500 ºC and a container temperature of 400 ºC, associated with a ram speed of 6.0 mm/s. Besides the extrusion process, the heat treatment is also a crucial part of the process for these 6xxx alloys. This process will be discussed and presented in the next section (2.2.2).

2.2.2. Heat Treatment

To maximise the mechanical properties of 6xxx AA, usually a T6 heat treatment is performed, involving a solution heat treatment and a further ageing heat treatment, as mentioned above.

2.2.2.1. Solution Heat Treatment

During casting, some intermetallic phases containing Fe are formed between the aluminium dendrites, as Al-Fe, Al-Fe-Si and Al-Fe-Mn-Si. The chemical composition of the formed phase depends on the cooling rate and the Fe:Si content ratio of the alloy, but the most commonly present phase is ß-AlFeSi, with the stoichiometry of about Al5FeSi [31].

The presence of such a phase significantly influences the forward processes, such as extrusion, since it reduces the ductility and workability of the alloy [31,32]. During SHT, the morphology of these particles is changed, and the ß-AlFeSi becomes α-AlFeSi, which has a rounded shape that allows better workability of the alloy [32,33,34].

During this process, there is also the dissolution of Mg_2Si and Si coarse particles formed during casting, which could cause tearing during extrusion [32].

A previous study [35] found that a small amount of Mn in 6063 AA significantly aids in homogenising and transforming the ß-AlFeSi phase into α-AlFeSi.

This process usually takes place at temperatures around 520 to 540 °C, allowing the dissolution mentioned above, and is followed by a quenching to keep the Si in solid solution, so that it can precipitate during the ageing treatment [15,19]. The quenching allows for the preservation of the vacancies formed during homogenization that assist in the precipitation during the ageing process [19].

About the SHT temperature, Nany *et al.* [19] studied the influence of ageing on the mechanical properties of 6063 AA and used a homogenisation temperature of 525 ºC for 2 hours, followed by ice-water quenching. On another approach, Silva *et al.* [36] used 540 ºC for 3 hours to solution heat treat 6063 AA, to analyse the influence of chemical composition on the mechanical properties after age-hardening. Demir *et al.* [23] used the same treatment conditions to study the effect of artificial ageing on the machinability of 6061 AA. All these conditions resulted in a solubilised microstructure, fulfilling the objective of this treatment.

Summing up, the final product of the SHT is a super saturated solid solution, which will represent the starting point to the ageing treatment, allowing the formation of the desired precipitates on the aluminium. These precipitates allow the maximum enhancement of the alloy. Figure 8 presents the microstructure of 6xxx AA before and after solution heat treatment [31].

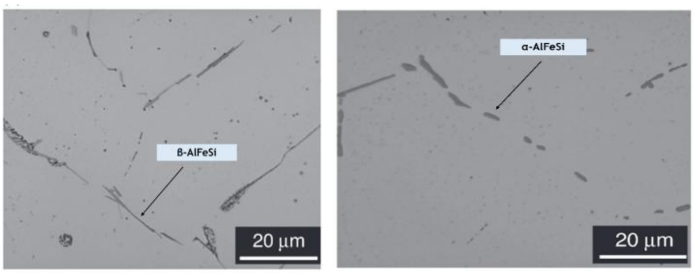

Figure 8: Microstructure of a 6xxx AA a) as-cast b) as-solubilised [31].

2.2.2.2. Ageing Heat Treatment

Artificial ageing heat treatment typically occurs after the SHT and extrusion processes, aiming to improve the mechanical properties of these alloys through the precipitation of Mg-Si particles. For this, the method employs temperatures ranging from 150 to 200 ºC [21].

This process allows the formation of Si initial clusters that attract Mg atoms, forming co-clusters. These particles turn to Guinier-Preston (GP) zones, which are believed to be spherical. After that, there is the formation of β'' precipitates, which are referred to as the stage that allows the maximum hardening and strengthening of the alloys [31,32,37,38].

The sequence of precipitation in 6xxx Al-Mg-Si systems can be expressed by the scheme presented in Figure 9 [39]:

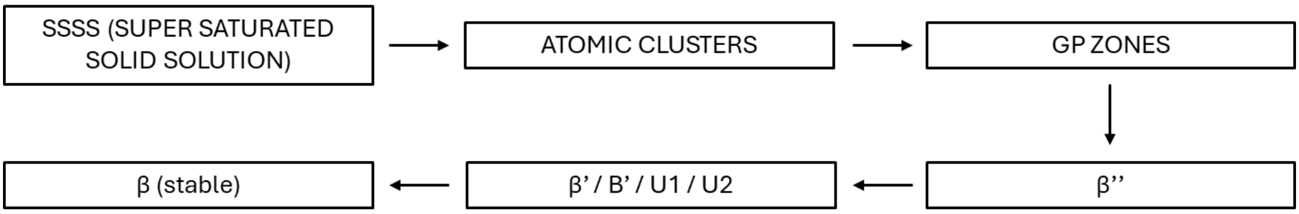

Figure 9: Precipitation sequence in 6xxx AA [39].

Figure 10 present a time-temperature-transformation illustrative diagram, where the combination of temperature and time of exposure after which a type of precipitate can be referred to as metastable is shown [40].

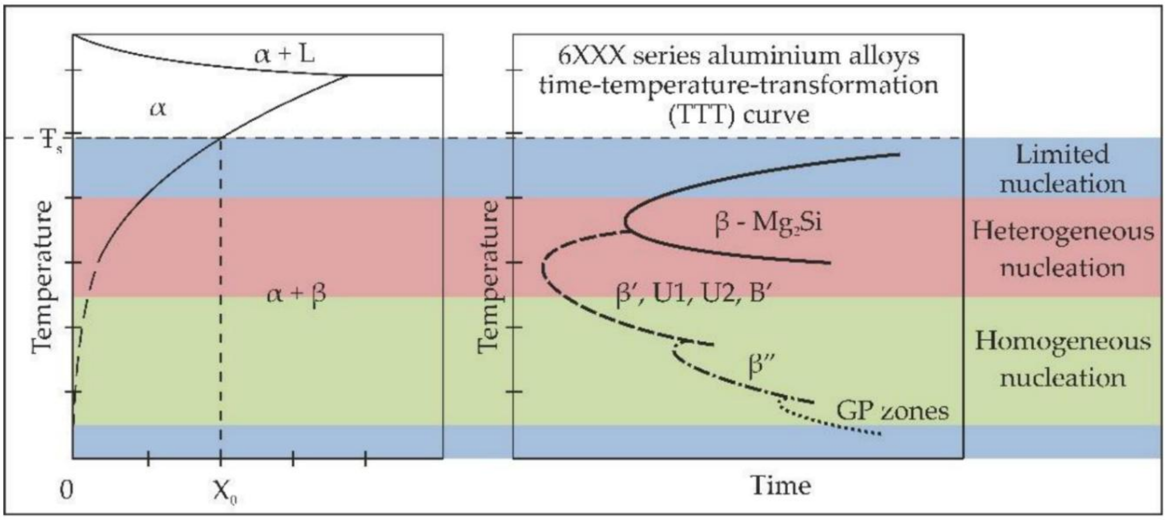

Figure 10: TTT diagram of the precipitation phases in 6xxx AA [40].

The chemical composition of the alloy, especially the Si/Mg ratio, and the ageing temperature, affect the composition of the precipitates formed during the ageing treatment [39]. Marioara *et al.* [39] showed that at an ageing temperature of 175 ºC, the main precipitates on the microstructure of alloys with Si/Mg ratios of 1.25 and 0.8 were ß'' and GP Zones at the peak hardness condition. The ß'' precipitates are the main hardening precipitates, and they nucleate at temperatures above 100 ºC and remain metastable until 200 ºC [40].

The shape and composition of the precipitation phases were studied before, and the results are presented in Table 8 [32,39].

Table 8: Shape and composition of the precipitation phases [39].

PHASE	SHAPE	STOICHIOMETRY
GP-zones	Needle	Mg_4AlSi_6
B''	Needle	Mg_5Si_6
B'	Needle	$Mg_{1.8}Si$
U1	Needle	$MgAl_2Si_2$
U2	Needle	MgAlSi
B'*	Lath	$Mg_9Al_3Si_7$*
B	Plate	Mg_2Si

The temperature and the duration of the ageing define the final mechanical properties of the alloy. Using lower ageing temperatures, the peak hardness is higher, but it requires a longer ageing time to achieve that condition. At lower temperatures, the diffusion of solute atoms is slower, allowing the formation of many small GP zones, which increase the density of fine precipitates. This phenomenon increases the obstruction to the dislocation motion, achieving a higher strength of the alloy [41]. For every temperature, there is a moment after which the strength of the alloy starts to decrease, and a process called overageing takes place, since the post ß'' metastable phases are formed [15].

About the influence of ageing time, Nandy *et al.* [19] studied the impact of ageing on the mechanical properties of a 6063 AA using an ageing temperature of 175 ºC and ageing durations from 10 minutes to 14 days. The peak hardness condition was reached at 8 hours of ageing. Also, Munitz *et al.* [20] used different ageing durations to find the peak hardness for a 6063 AA, evaluating the tensile properties. The peak strength was reached at 24 hours, but only with slight differences in the values for the 8, 16 and 20-hour samples. The effect of temperature for the same duration was also studied, using temperatures of 150 ºC to 240 ºC, with a step of 10 ºC, and an ageing duration of 5.5 hours. The results showed that the strength of the alloy increased (230 to 251 MPa) with increasing temperature until 195 ºC and decreased after that, showing that with rising temperatures, the peak hardness happens sooner than with lower ageing temperatures. Still, the use of lower ageing temperatures allows for achieving higher peak hardness and strength [20].

He *et al.* [42] examined how ageing temperature and ageing time affect the mechanical properties of 6063 AA. Three different temperatures (150, 175, and 190 ˚C) were tested for up to 38 hours. The results indicated that the highest hardness and strength were achieved at 150 °C, with optimal properties at around 36 hours of ageing.

For 175 °C, the peak occurred at 11 hours of ageing. At 150 °C, the maximum strength was 231 MPa, whereas at 190 °C, it was 209 MPa after 4 hours of ageing. These findings are shown in Figure 11.

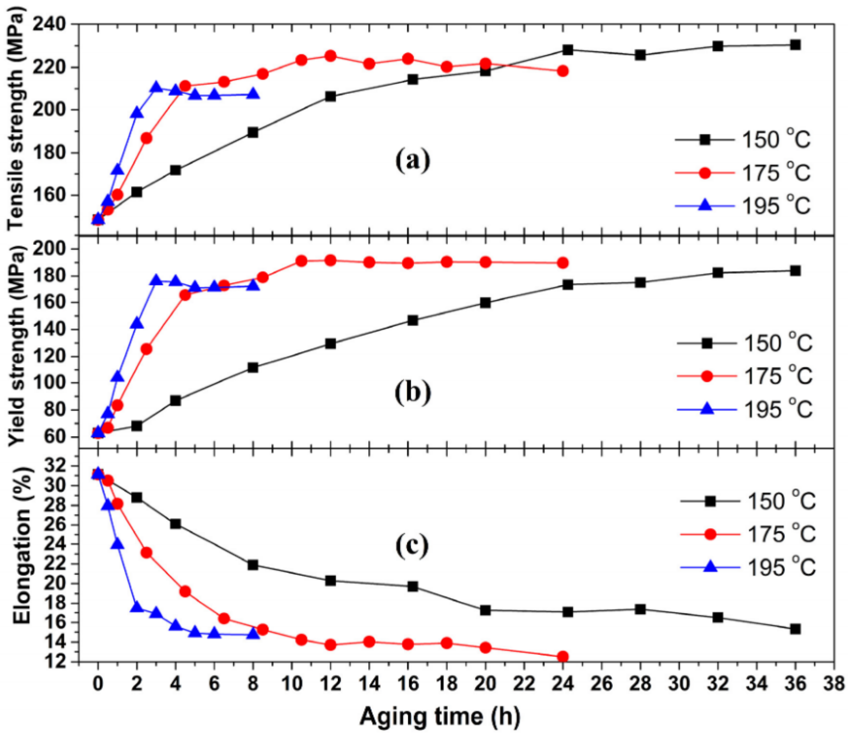

Figure 11: Influence on ageing temperature and time on the mechanical properties of a 6063 AA [42].

Menapace *et al.* [16] studied the possibility of using dual-rate and dual-step ageing treatments. The first one consists of using a first quick heating rate to reach an intermediate temperature, followed by a slower rate until the final ageing temperature. On the other hand, the dual step process consists of heating the material to an intermediate temperature, holding it there for a defined time, and then heating it slowly to the final temperature. The results showed that these processes allow for achieving higher hardness values with shorter ageing times and that, at the peak condition, Mg_5Si_6 particles were revealed through TEM analysis. The use of an intermediate temperature, lower than the typical used on the conventional ageing treatments, promotes a fine and dispersed nucleation of GP zones and β'' precipitates. These are the particles that allow the maximum hardening of the alloy, and then, when a higher temperature is applied, these particles will grow while maintaining their fine dispersion and allowing the peak hardness condition to be achieved in significantly shorter times [43,44].

Summing up, the optimisation of both ageing temperature and ageing time is crucial for the maximum enhancement of the mechanical properties of the alloy.

2.3. Ladders Industry and its Regulation

The ladder industry must adhere to specific requirements to obtain product approval. The European Standard EN 131 sets out the requirements, testing conditions, and markings for ladders on the market. This standard outlines different requirements for the ladder's response to strength tests, depending on whether the ladder is intended for professional use. It applies to all ladder parts and types, including leaning ladders, standing ladders with a platform, combination ladders, and standing ladders. For non-professional use, the standard specifies that the ladder must support a load of 2250 N, whereas for professional use, this increases to 2700 N.

Following this standard and having a positive response to those tests, a ladder can be approved and sold in the market.

3. EXPERIMENTAL PROCEDURE

The experimental procedure of this work can be split into five stages, as shown in Figure 12: analysis of the 6060 and 6061 AA profiles in the as-received condition, i.e., produced using the supplier's traditional heat treatment parameters; production of ladders with profiles from three different dual ageing conditions; study of how the ladder's manufacturing process affects its failure mechanism; analysis of the influence of ageing parameters on the mechanical properties of the alloy; and analysis of the mechanical performance of 6060 and 6061 AA ladders.

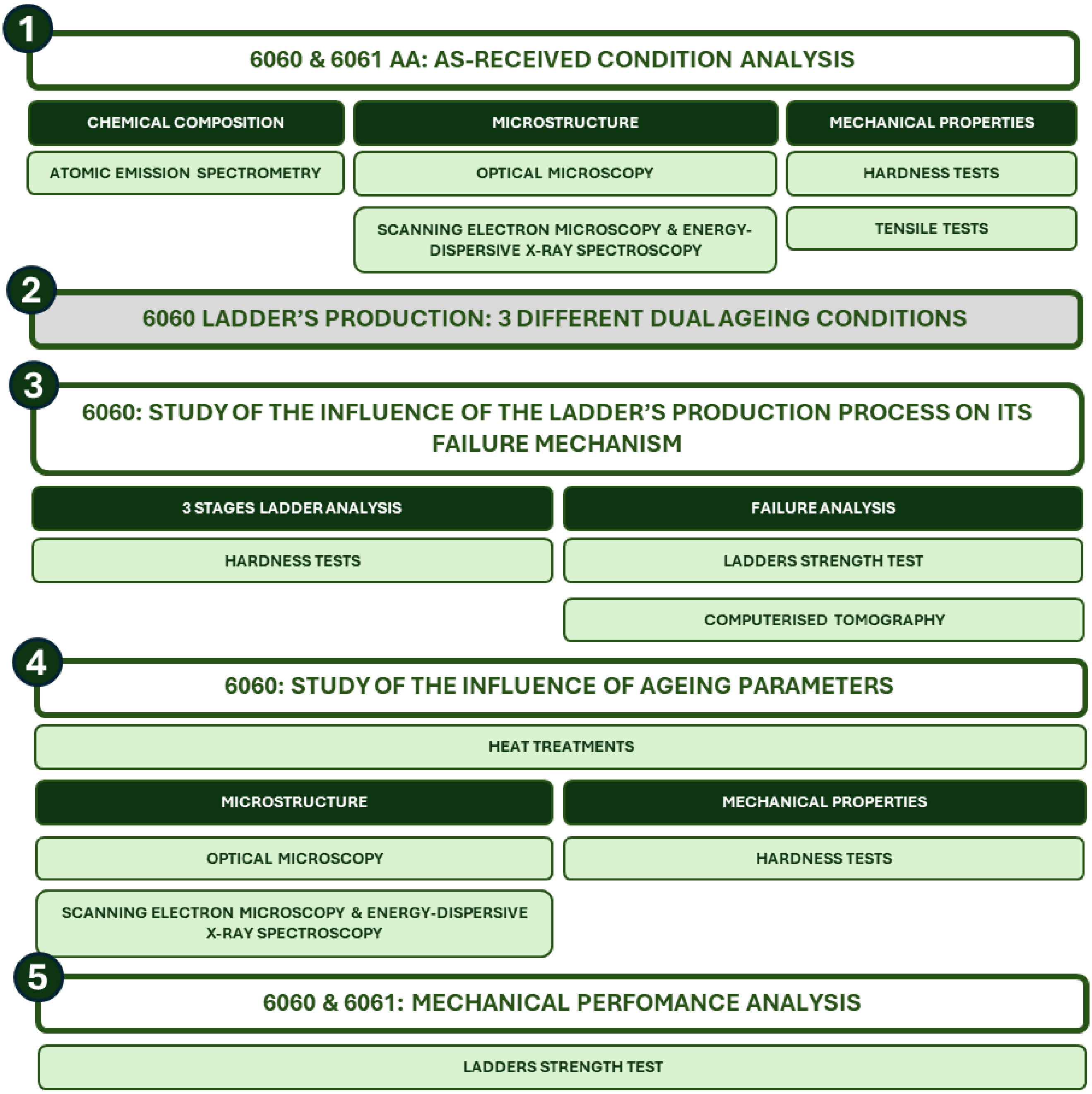

Figure 12: Scheme of the experimental procedure.

3.1. Material

In this study, two different 6xxx AA, 6060 and 6061, were used to examine the influence of both heat treatment optimisation and production processes on the mechanical properties and performance of the ladders.

Both alloys were initially used in their as-received condition, produced by hot and direct extrusion with the supplier's usual heat treatment conditions. The chemical compositions, according to the supplier's certificate, are presented in Tables 9 and 11.

The 6060 AA was also used in its as-extruded condition, without any subsequent heat treatment, with the chemical composition presented in Table 10.

These alloys were always received and tested using two different profiles to understand if the shape factor of the profile was also a significant parameter in the ladder performance. The technical drawings of the used profiles are presented in Figure 13.

Table 9: Supplier's certificate composition of the 6060 AA.

6060 AA: CHEMICAL COMPOSITION										
ELEMENT	Al	Cr	Cu	Fe	Mg	Mn	Si	Ti	Zn	Others
WEIGHT %	-	< 0.01	< 0.01	0.21	0.38	0.02	0.45	0.01	< 0.01	-

Table 10: Supplier's certificate chemical composition of the 6060 AA as-extruded.

6060 AA AS EXTRUDED: CHEMICAL COMPOSITION										
ELEMENT	Al	Cr	Cu	Fe	Mg	Mn	Si	Ti	Zn	Others
WEIGHT %	98.71	0.00	0.00	0.20	0.52	0.02	0.53	-	0.012	-

Table 11. Supplier's certificate chemical composition of the 6061 AA.

6061 AA: CHEMICAL COMPOSITION										
ELEMENT	Al	Cr	Cu	Fe	Mg	Mn	Si	Ti	Zn	Others
WEIGHT %	98.06	0.06	0.20	0.20	0.81	0.03	0.61	0.00	0.01	0.02

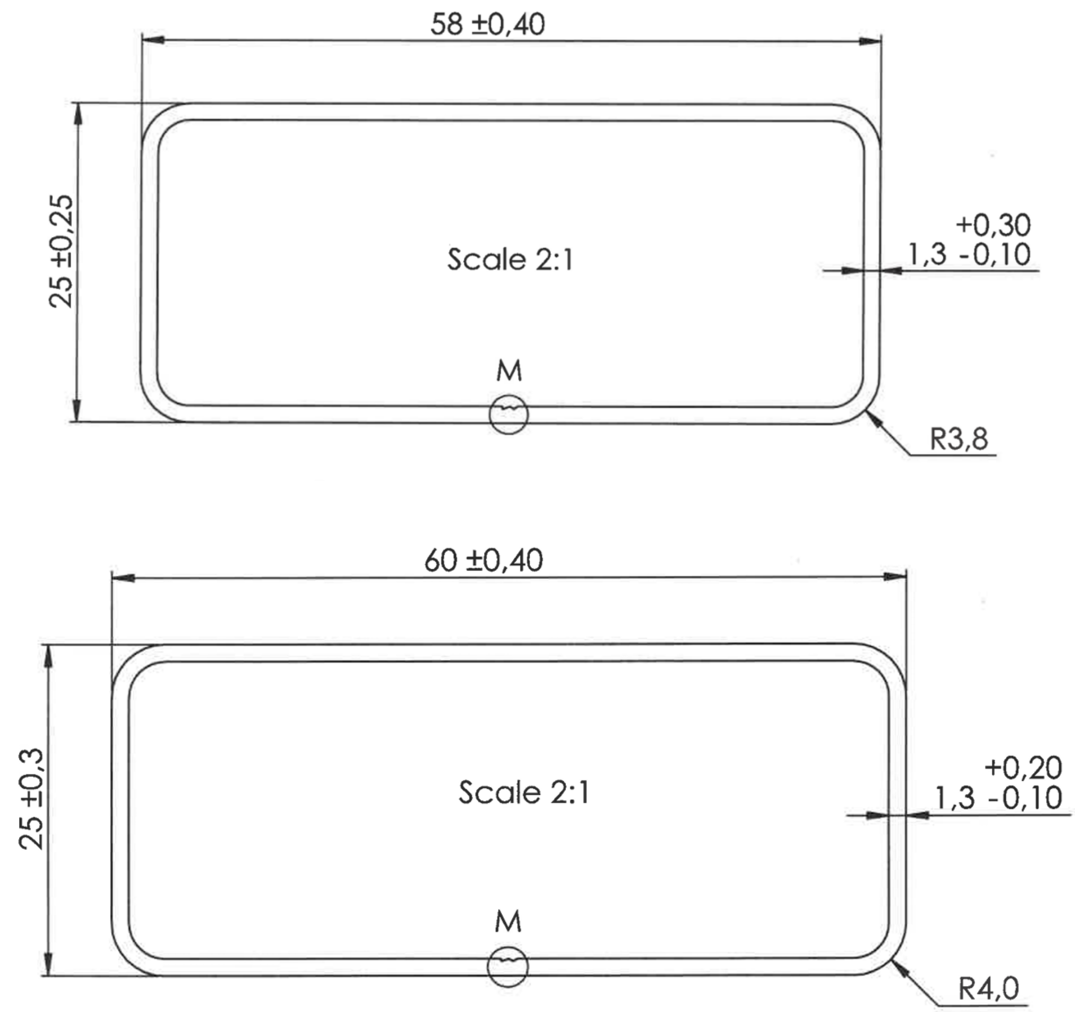

Figure 13: Technical drawings of the ladders' lateral profiles (mm).

3.2. 6060 and 6061 AA as-received analysis

At the start of this study, both alloys were characterised in their as-received condition. First, the chemical composition was assessed using Atomic Emission Spectrometry (AES) and the results were compared to the values provided by the suppliers to verify the content of the main alloying elements, Mg and Si.

After that, to understand how the elements were arranged in the microstructure, a sample of each alloy was prepared metallographically for analysis using optical microscopy (OM) SEM and energy-dispersive X-ray spectroscopy (EDS). To characterise these alloys and their heat treatment conditions in terms of their mechanical properties, hardness (Vickers and Brinell), and tensile tests were performed. The tensile tests were performed on specimens taken from the longitudinal section of 25 mm samples of the profiles. From each profile sample, two specimens were produced, one from the top section and other from the lower section. Three tests were conducted for each condition.

3.3. 6060: Different Dual Ageing Conditions

After the analysis and characterisation outlined above, the study focused on the 6060 AA. The supplier's typical ageing heat treatment involves initially heating the material to an intermediate temperature of 150 °C, followed by a holding stage at the same temperature. Subsequently, the profiles are heated to the final ageing temperature and maintained there for an extended period. To examine the effect of different ageing temperatures and durations on the mechanical properties and performance of 6060 AA, other dual ageing (DA) conditions were tested. The final ageing temperature and the total ageing time were the varying parameters in this study.

Ladders were produced using profiles from these three different conditions for mechanical testing, and longitudinal samples were prepared metallographically for microstructural analysis and hardness testing, using the Vickers method. The microstructural analysis was performed by using OM, SEM and EDS analysis. The results were compared to those of the standard simple ageing treatment, which will be presented in section 3.5. The variable parameters used in these three other conditions are shown in Table 12.

Table 12: Conditions and parameters of the dual ageing treatments.

DUAL AGEING PARAMETERS		
CONDITION	FINAL AGEING TEMPERATURE (°C)	TOTAL AGEING TIME (h)
DA 1	185	4,5
DA 2	185	6
DA 3	195	6

3.3.1. Ladder's Production Process

The production of these ladders involves several steps, as shown in Figure 14. The first three steps are the most critical, as they are performed on the profiles, directly depending on their mechanical properties and heat treatment conditions. These are the stages during

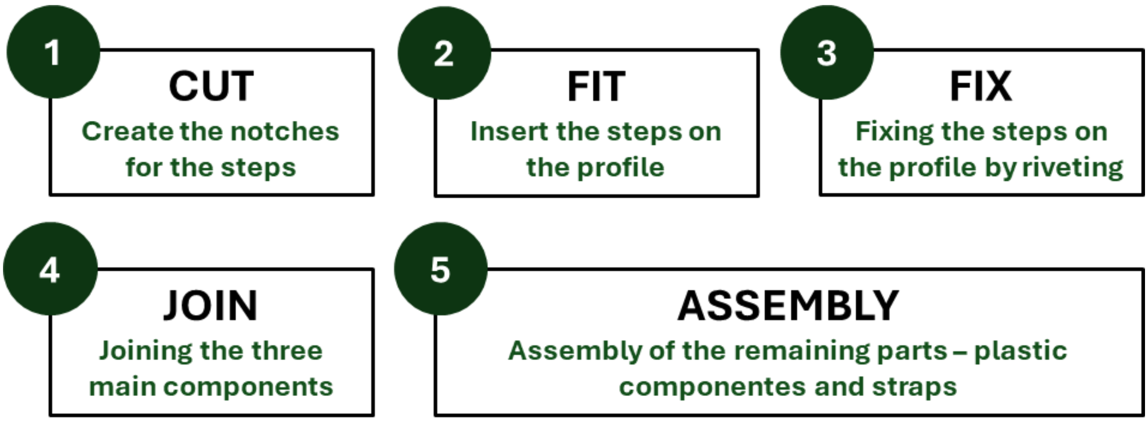

Figure 14: Scheme of the ladder's production process.

which the process can influence the failure mechanism, which will be further analysed to understand its influence.

The first three and most critical stages of this process are all carried out in a single equipment. The first stage involves the cutting of the lateral profile of the ladder, performed by punching a die into the profile. After that, the step is fitted in place, followed by its fixation through a bending action applied to the outer area of the profile. The fourth stage includes the coupling of the three ladder components, since it is a triple ladder, and the process is finalised with the placement of the remaining parts, as straps and plastic components.

3.4. 6060: Study of the Influence of the Ladder's Production Process

The reasons for failure and their mechanisms are key points to analyse and understand. To determine whether the production process was the cause or could increase the likelihood of occurrence, a study was conducted on the first three steps of that process. To aid this, a ladder was produced with three different zones, as shown in Figure 15. These zones were examined through hardness tests using the Vickers method with a load of 100 gf. The indentations were made 0.5 mm apart from each other, starting from the cut vertex outward along the diagonal of the cut, as also shown in Figure 15.

The hardness values of the three zones were compared to evaluate whether they increased as the process progressed. This analysis was conducted because the manufacturing process of the ladders involves material deformation, which may result in strain hardening. Such strain hardening enhances the material's brittleness, a characteristic also indicated by elevated hardness values [45].

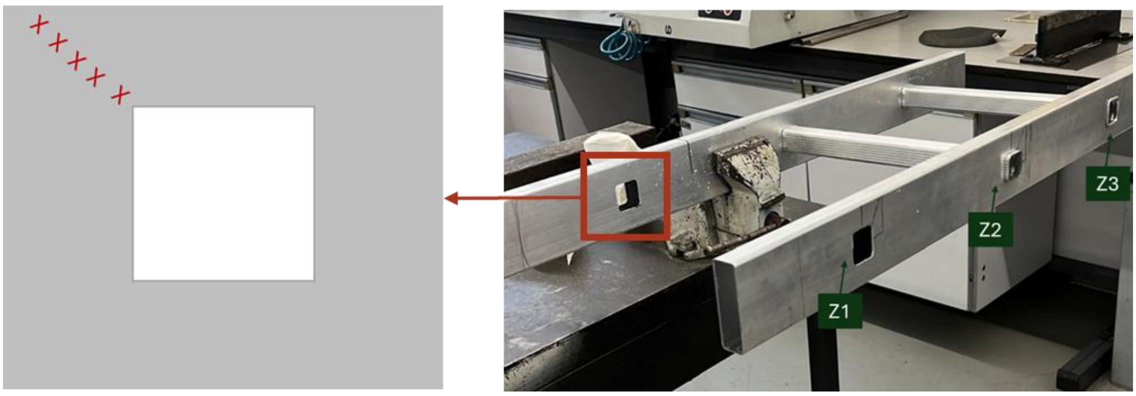

Figure 15: Representation of the a) hardness tests' profile b) ladder with three different zones.

Regarding the failure mechanism analysis, ladders with the three different ageing conditions and two different profiles were tested on the Ladders' Strength Test, as suggested by the EN 131-2+A2:2017 standard. Their failure zone was cut and studied by Computerised Tomography (CT). The designation attributed to each heat treatment condition and profile length is presented in Table 13.

Table 13: Conditions used on the CT analysis.

DESIGNATION	PARAMETERS		
	FINAL AGEING TEMPERATURE (°C)	TOTAL AGEING TIME (h)	WALL THICKNESS (mm)
DA1.58	185	4.5	58
DA2.58	185	6	58
DA1.60	185	4.5	60
DA3.58	195	6	58
DA3.60	195	6	60

3.5. Study of the Influence of Ageing Parameters

To maximise the mechanical performance of the ladder, by maximising its hardness and strength, it is essential to reach the peak strength heat treatment condition. To accomplish this, heat treatments were carried out at 175 °C, a temperature selected based on a study, the results of which are presented in Appendix B.

This study used the as-extruded 6060 profiles, which underwent SHT at 520 °C for 2 hours and were then cooled with forced air, as the supplier's cooling system. After the solution heat treatment (SHT), the samples were kept in a freezer at -20 °C to avoid any natural ageing. Different ageing times were tested with a 2-hour step, from 2 to 20 hours. These heat treatments took place in an air ventilated muffle furnace, different from those of the supplier’s heat treatments.

For each condition, a sample was metallographically prepared. Hardness tests were conducted by performing five indentations per specimen. The microstructure of the as-solubilised specimen and the maximum hardening condition specimen were also analysed through OM, SEM and EDS analysis to understand the microstructure characteristics and the chemical composition and morphology of the present precipitates.

These samples were compared to the DA ones, since it was critical to determine if DA allows for achieving the same mechanical properties with shorter ageing times, and if there are any differences in the microstructure.

3.6. Ladders’ Mechanical Performance Analysis

As a final step, the mechanical performance of the ladders was tested and analysed using the Ladders’ Strength Test, as described in section 5.3. This analysis included the 6061 AA in the as-received condition for both profiles, based on the results of the 6060 AA tests.

3.7. Equipment, standards and specifications

This section presents all the specifications used in the experimental procedure, including the equipment and standards employed, presented in Table 14. The metallographic preparation specifications and process are also presented in this section.

Table 14: Equipment and standards used for each analysis.

ANALYSIS / TEST	EQUIPMENT	STANDARD
ATOMIC EMISSION SPECTROMETRY	SPECTROLAB LACM12	-
OPTICAL MICROSCOPY	Leica DM4000M	-
SEM / EDS*[1]	FEI Quanta 400 FEG with an EDAX Genesis X4M EDS	-
COMPUTERISED TOMOGRAPHY	Metrotom 15000	-
VICKERS HARDNESS TEST (HV 0.1)*[2]	FALCON 400 micro/macro-Vickers hardness tester (INNOVATEST)	ISO 6507-1:2005
VICKERS HARDNESS TEST (HV 10)	DuraVision G5 EMCOtest	ISO 6507-1:2005
BRINELL HARDNESS TEST (HB 2.5/31.25)	DuraVision G5 EMCOtest	ISO 6506-1:2009
TENSILE TESTS	SHIMADZU UH1000kNX	NP EN ISO 6892-1:2022
LADDERS STRENGTH TEST	-	EN 131-2:2010+A2:2017

*[1] only used on the as-received condition analysis.
*[2] only used on the influence of the production process.

The metallographic preparation of all the samples involved using polishing with silicon carbide abrasive papers with the following grits sequence: 180, 320, 600, 1000 and 4000 mesh. After that, the specimens were polished with diamond suspensions of 6 and 1 μm, and colloidal silica of 0,6 μm. To guarantee a better surface finishing, the specimens were also polish with a colloidal silica with ammonia and hydrogen peroxide solution for two minutes. To allow the microstructural analysis, the specimens were chemically etched with Weck's reagent for eight seconds.

4. RESULTS AND DISCUSSION

This chapter will include the results and its discussion. The organization will follow the same presented in experimental procedure (Figure 12), being divided in: (1) as-received condition analysis; (2) influence of ladder's production process analysis; (3) influence of ageing parameters; and (4) ladders' mechanical performance analysis. An additional section about the measures that should be acquired by the company on its raw material control and inspection will also be presented in this chapter.

4.1. As-received Condition Analysis

6060 and 6061 AA were analysed in their as-received condition, being characterised on their chemical composition, microstructure and mechanical properties.

4.1.1. Chemical Composition Analysis

The results of the AES analysis performed on the as-received samples are shown in Table 15, next to the supplier's certificate values, to allow a better comparison between them.

Table 15: Results of the AES analysis.

ELEMENT	6060		6061	
	SUPPLIER'S CERTIFICATE (WEIGHT%)	AES RESULTS (WEIGHT%)	SUPPLIER'S CERTIFICATE (WEIGHT%)	AES RESULTS (WEIGHT%)
Cr	< 0.01	< 0.006	0.06	0.063 ± 0.008
Cu	< 0.01	< 0.01	-	< 0.01
Fe	0.21	0.203 ± 0.024	0.2	0.197 ± 0.024
Mg	0.38	0.502 ± 0.06	0.81	0.776 ± 0.093
Mn	0.02	0.021 ± 0.003	0.03	0.039 ± 0.05
Si	0.45	0.51 ± 0.066	0.61	0.587 ± 0.076
Ti	0.01	< 0.01	0	< 0.01
Zn	< 0.01	< 0.02	0.01	< 0.02
Bi		< 0.02		< 0.02
Ni		0.005 ± 0.001		< 0.004
Pb		< 0.002		< 0.002
Sn		< 0.0008		< 0.0008
V		0.009 ± 0.001		< 0.005
Zr		0.001 ± 0.0002		0.001 ± 0.0001

Results from the 6060 AA confirm the chemical composition provided by the supplier, as the values obtained through AES analysis were very similar to those from the supplier, except for Mg. This value was significantly higher than the expected content (0.50 to 0.38%), highlighting the importance of this control, since a different content of Mg or Si will lead to a different ratio between them. As mentioned in the literature review (section 2.1.5), the stoichiometry of the precipitates also depends on the Mg/Si ratio. This means that with better control of the chemical composition, especially of the content of these two elements, it's easier to predict the precipitates formed to achieve the maximum strengthening of the alloy and the product. It's also possible to see that the chemical composition of this alloy fits both 6060 and 6063 AA theoretical chemical compositions presented in the previous literature review (section 2.1.6). For this reason, both alloys' mechanical properties should be considered in comparison to the peak condition achieved in this work, to determine if the peak hardness expected for these alloys was achieved.

Concerning the 6061 AA, the AES analysis verified the contents supplied by the supplier for all of the elements. It highlighted that the Mg and Si contents, crucial for maximum hardening and enhancement, were highly consistent with those derived from this analysis.

4.1.2. Microstructural Analysis

Regarding the microstructure of both alloys, Figure 16 shows the microstructures of 6060 and 6061 AA in their as-received conditions.

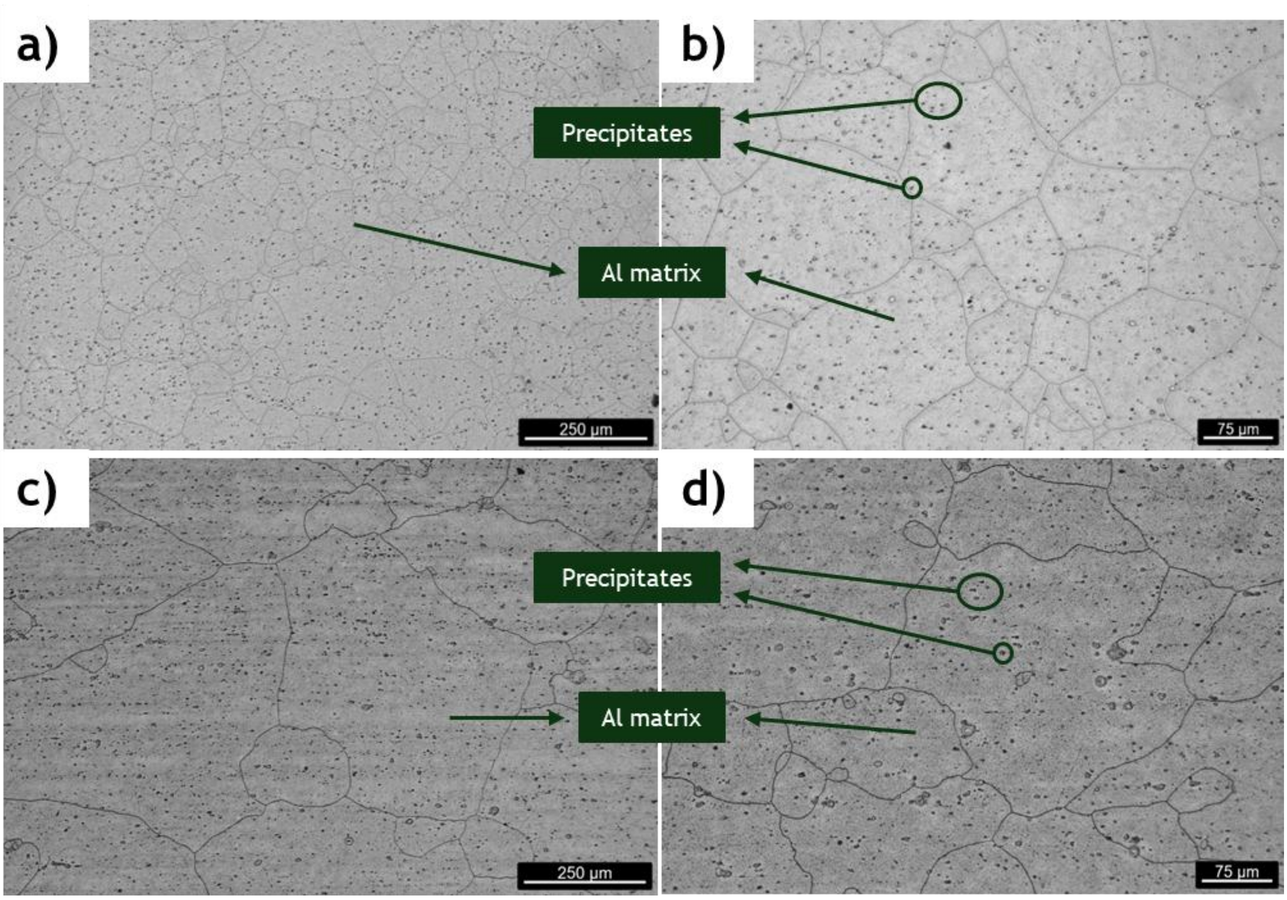

Figure 16: Microstructure of a) 6060 AA as-received b) with a higher magnification c) 6061 as-received d) with a higher magnification.

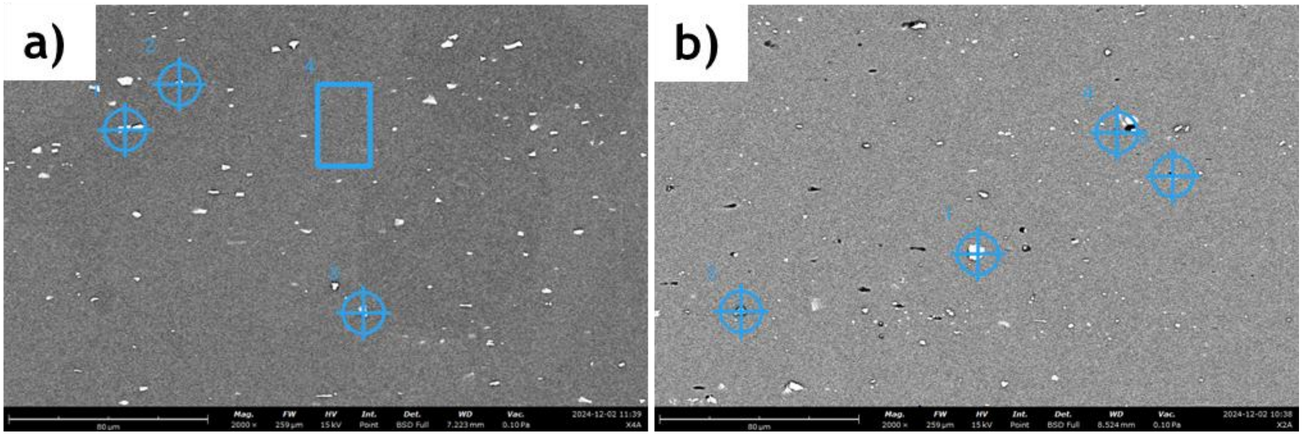

Figure 17: SEM images of the microstructure of a) 6060 AA as-received b) 6061 AA as-received.

Both microstructures exhibit a clear Al matrix characterised by well-defined grains of markedly varying sizes within the same alloy.

Figure 16 demonstrates that the 6061 AA displays larger grains within its microstructure, which, in accordance with the Hall-Petch relationship, results in reduced hardness and strength values, given that grain boundaries serve as impediments to dislocation motion [46]. Nonetheless, the increased concentration of alloying elements, theoretically, provides this alloy with better mechanical properties compared to the 6060 AA, a point that will be further analysed in the following section. The 6061 AA microstructure also shows grain boundaries with more irregular and pronounced contours when compared to the 6060 AA. This can also be attributed to the higher concentration of alloying elements, particularly Cu, that can lead to the formation of other precipitates that block the grain boundaries, giving them these more pronounced contours [47].

Additionally, a substantial presence and density of precipitates of various sizes are observable, especially in Figure 17. According to the EDS analysis, these particles correspond to precipitates formed during cooling and SHT stages, comprising Al, Fe, Si. This microstructural analysis, using OM and SEM/EDS, allowed for a better understanding of the differences between the 6060 and 6061 AA structures and for further knowledge and validation of the post-ageing microstructure of these alloys. As a notable example, it was possible to confirm that the AlFeSi precipitates remain in the structure after the SHT and ageing treatment, acquiring a rounded and less fragile morphology.

As previously mentioned (section 2.2.2.2), the hardening precipitates, containing Mg and Si, are generally much smaller, requiring more advanced observation techniques, as TEM, to validate their existence and to analyse their stoichiometry, density, and dimensions [48,49].

4.1.3. Mechanical Properties

In this study, the hardness and tensile properties of both alloys were analysed to characterise them and to allow further comparison values with subsequent studies (section 4.3). The results are presented in Tables 16 and 17.

Table 16: Results of the hardness tests of the as-received specimens.

ALLOY	VICKERS HARDNESS (HV 10)		BRINNEL HARDNESS (HB 2,5 / 31,25)	
	Mean	Standard Error	Mean	Standard Error
6060	88	3	82	± 1
6061	100	1	93	± 1

Table 17: Results of the tensile tests of the as-received specimens.

ALLOY	Rp 0.2 (MPa)		Rm (MPa)		ELONGATION (%)	
	Mean	Standard Error	Mean	Standard Error	Mean	Standard Error
6060	243	5	263	5	12	± 1
6061	269	8	288	7	10	± 0

6061 AA demonstrated higher hardness and tensile strength values. These findings are consistent with the expectations based on the literature review (section 2.1.6.3), given that this alloy contains a greater concentration of alloying elements relative to 6060. The increased Mg content enhances hardness and tensile strength but results in reduced ductility and toughness [21]. This is further corroborated by the fact that the elongation of 6060 AA surpassed that of 6061. These results also show that the precipitating hardening influence surpasses the grain refinement mechanism influence, since even with a bigger grain size, the 6061 AA achieves higher mechanical properties. For ladder applications, ductility and toughness constitute vital properties, as material failure should be gradual and perceptible rather than brittle. Nonetheless, the 2% variation is not substantial in this context, placing both alloys within a comparable range concerning these properties.

4.2. Influence of Ladder's Production Process Analysis

As previously outlined, to assess the impact of the ladder's manufacturing process on its mechanical properties and performance, two distinct methodologies were employed: the first entailed producing a ladder with three different zones corresponding to the initial three critical production stages and performing hardness tests; the second involved analysing the failure zone through CT analysis conducted on five different ladders, with different dual ageing treatments conditions and profiles.

4.2.1. Hardness Tests

The results of the hardness tests conducted in the three distinct zones are illustrated in Figure 18.

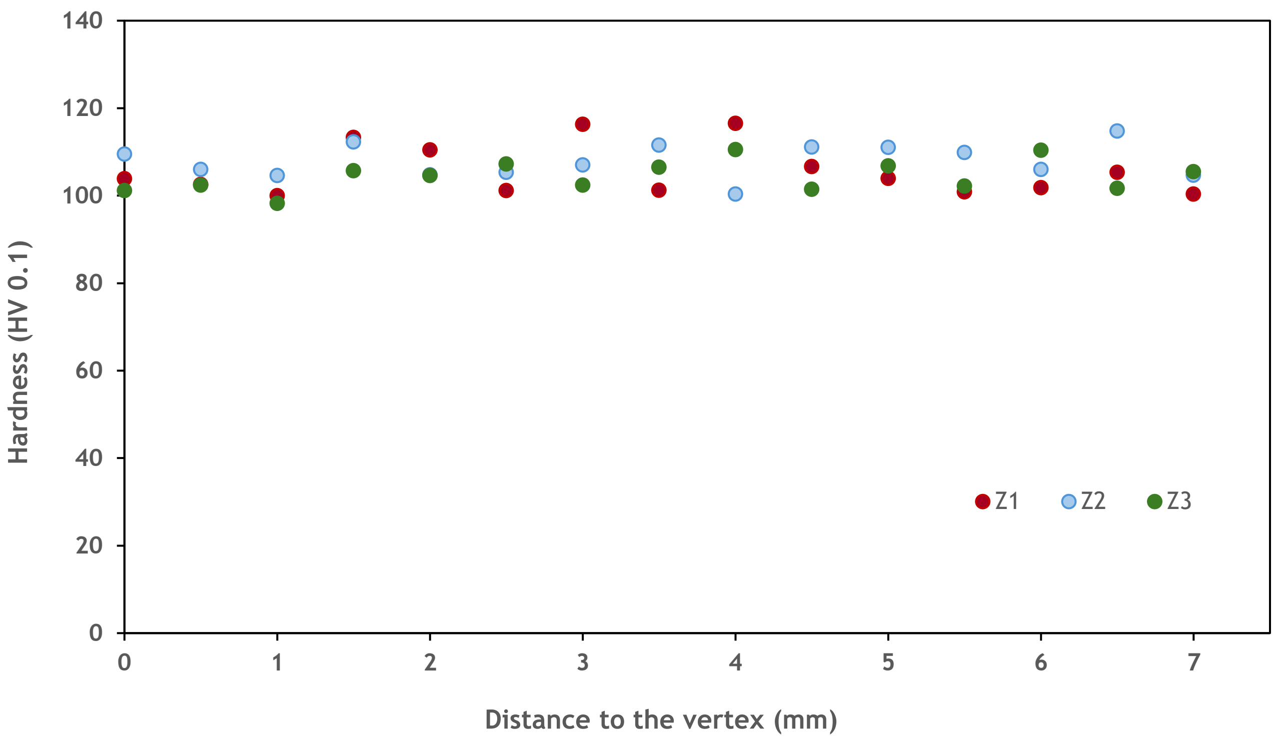

Figure 18: Influence of production process on the hardness of the profiles.

The analysis of these results highlights the absence of significant variation in the results, particularly relevant in the zones closer to the vertex, since they correspond to regions most directly subjected to the production process, such as cutting, fitting, and fixation of the step. The mean values overlap, falling within the range defined by the standard error associated with each mean.

The hardness values are slightly higher than those of the profile from which the ladder was produced. However, this can be attributed to the performance of the entire production process, resulting in strain hardening throughout the ladder itself.

These findings suggest that the production process does not significantly influence the material failure, as it does not promote substantial strain hardening in specific zones and, consequently, does not contribute to the material embrittlement. Nevertheless, this point should be complemented by the remaining analyses, especially the investigation of the failure mechanism, to confirm or refute this assumption.

However, as a suggestion for improving this analysis, applying a higher load would enable the determination of hardness values that could be more representative of the overall behaviour of the different zones, while potentially reducing the standard deviation associated with each zone.

4.2.2. Failure Mechanism Analysis

The failure mechanism was analysed using five ladders with different profiles and heat treatment conditions that failed the Ladders' Strength Test. The test result will be discussed later in this document, as a final step. Figures 19 to 23 present the results of the CT analysis for the five ladders from DA1.58 to DA3.60.

Figure 19: CT images of the DA1.58 profile (185 ºC, 4.5 hours and 58 mm).

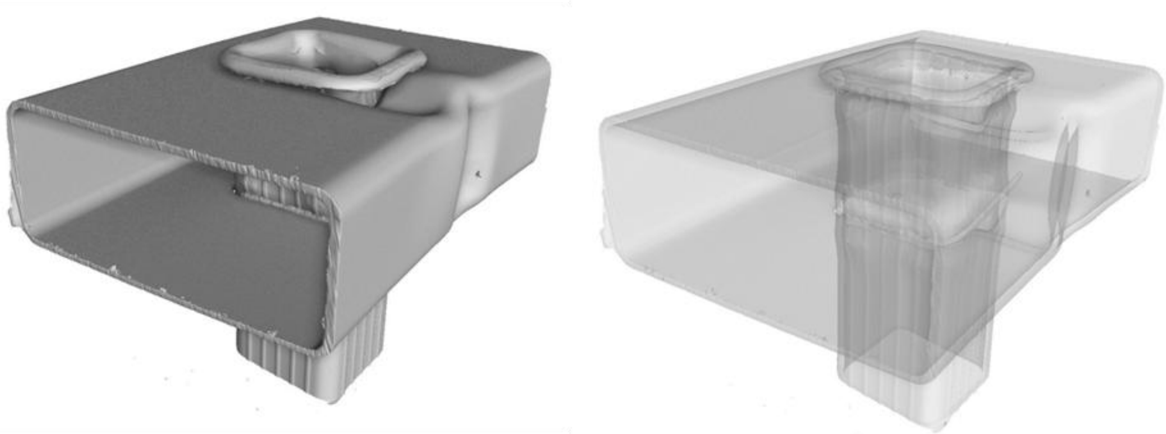

Figure 20: CT images of the DA1.60 profile (185 ºC, 4.5 hours and 60 mm).

Figure 21: CT images of the DA2.58 profile (185 ºC, 6 hours and 58 mm).

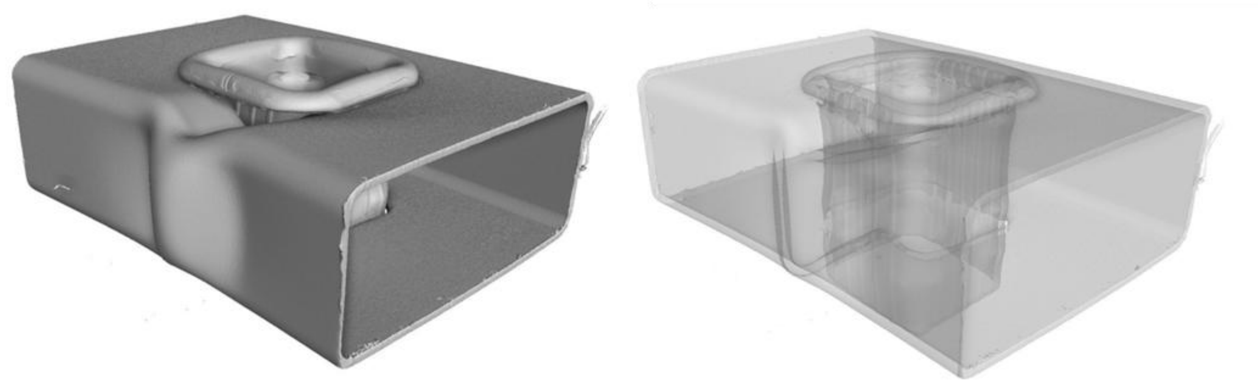

Figure 23: CT images of the DA3.58 profile (195 ºC, 6 hours and 58 mm).

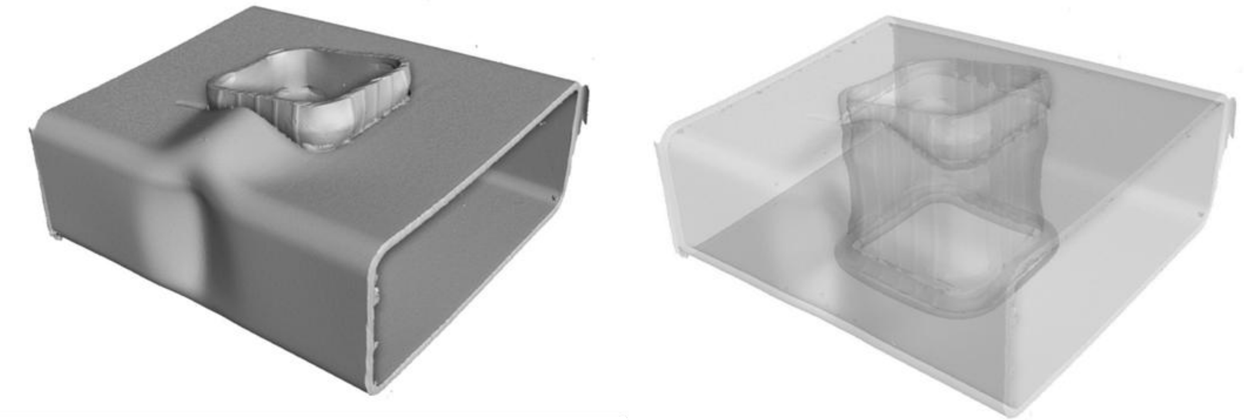

Figure 22: CT images of the DA3.60 profile (195 ºC, 6 hours and 60 mm).

Alongside providing images of the fracture zones, the CT analysis enabled the detection of discontinuities or cracks larger than 0.150 mm, due to the limited resolution of the equipment for the size of the zone to be analysed. These discontinuities were not found in any of the examined samples. This indicates that failure occurs solely through plastic deformation mechanisms, with no involvement of defective or brittle components. Additionally, the analysis findings demonstrate that failure morphology depends on the length of the cross-section of the profile. The 58 mm profiles showed failure as a depression in that area, whereas the 60 mm profiles showed failure characterised by a bulge in the same region.

A more comprehensive analysis in this regard could entail delineating a more precise zone of the failure area to facilitate the use of higher resolution imaging, thus enabling the verification of smaller discontinuities.

The findings of this study, which aimed to assess whether the manufacturing process affects the ladder's performance, are of considerable significance, since this insight can enable the company to obviate the necessity of testing new techniques at each production stage solely to ensure compliance with standards. Although such modifications and evaluations are beneficial for enhancing product quality, this study has demonstrated that the manufacturing process does not substantially impact the product's performance.

4.3. Influence of Ageing Parameters

As previously indicated, the effect of ageing parameters was examined through heat treatments, followed by assessing mechanical properties via hardness testing and microstructural analysis of the most pertinent heat treatment conditions. These findings were subsequently compared with those from identical evaluations of specimens subjected to various dual ageing treatments to establish a correlation between the parameters and the final properties of the material.

4.3.1. Hardness Tests

The results of the hardness tests are presented in Figure 24.

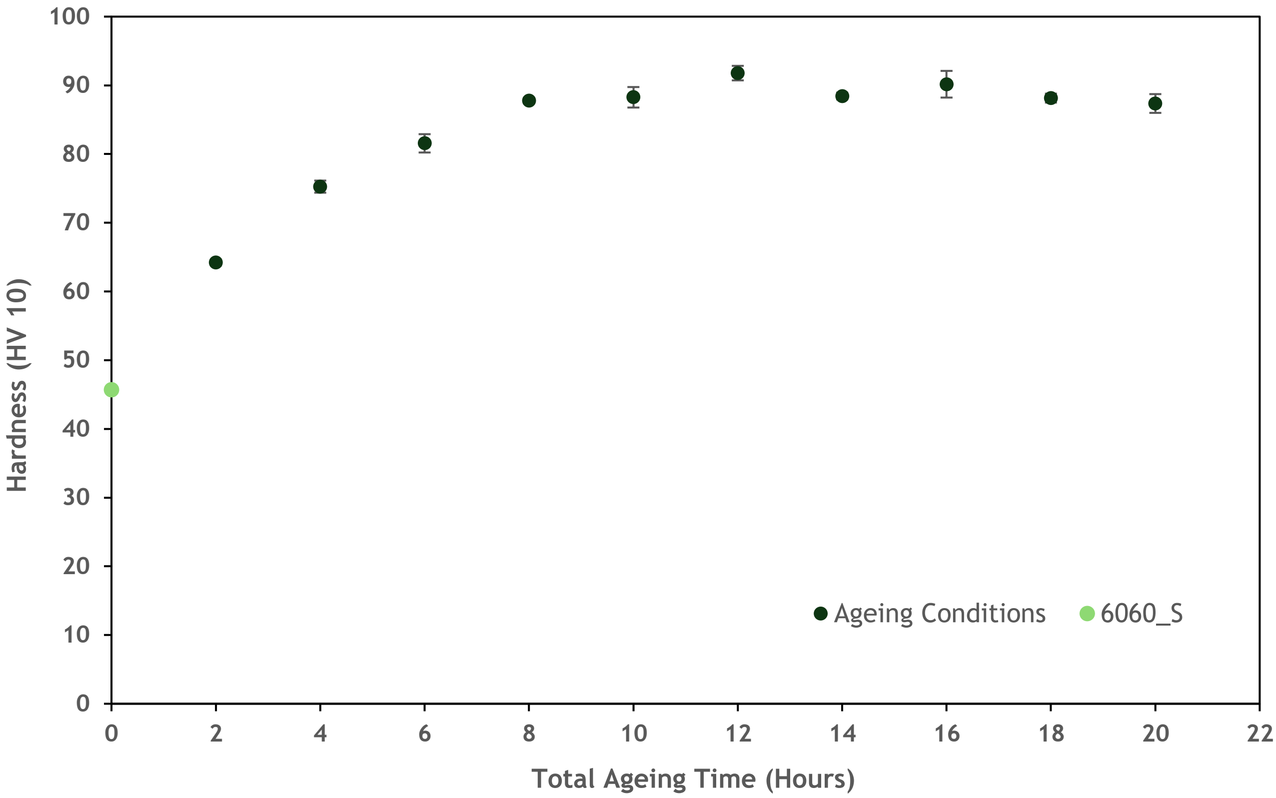

Figure 24: Influence of ageing time at 175 ºC on the hardness of the 6060 AA.

The curve of hardness values for each heat treatment confirms the effectiveness of the ageing process. The hardness of the specimen aged for the shortest time (2 hours) is notably higher than that of the 6060_S specimen, since the hardness increased from 46 to 64 HV.

As anticipated and corroborated by previous studies [19,20,42], an increase in ageing durations significantly enhanced the material's hardness, and the maximum hardness condition, of 92 HV, was attained at 12 hours of treatment. Subsequently, the overageing phenomenon occurs, leading to a deterioration in the material’s mechanical properties. However, an anomaly was observed post-peak, whereby the 16-hour sample exhibited a higher hardness value than the 14-hour sample. Although this outcome was unexpected, the slight variations in results between different conditions suggest that minor inconsistencies in the treatment process may be responsible for these anomalies. Due to the relatively low temperatures in this type of treatment, combined with the limited precision of the oven's temperature control, variations in temperature occurred at the beginning of the treatment. Opening the oven to insert the samples caused a slight temperature drop, which rebounded after closing. Nonetheless, due to the oven's insensitivity to the actual temperature fluctuations, the temperature often overshot the set point. Consequently, the temperature achieved during heating was variable, thereby contributing to a minor error in the resulting data, which can explain the 16-hour anomaly in the hardness value.

These results showed that the peak hardness condition is found at longer times than those achievable by the supplier in this study. This makes DA a crucial option for reaching this condition. However, to verify the potential success of this option, a comparison was made between the peak hardness condition and the samples provided with different DA treatments.

Table 18: Results of the hardness tests on specimens with different ageing treatments.

SAMPLE	TYPE OF AGEING	FINAL AGEING TEMPERATURE (°C)	TOTAL AGEING TIME (h)	HARDNESS (HV10)	
				Mean	Standard Error
6060_S	-	-	-	46	± 1
6060_12h	Conventional	175	12	92	± 1
6060_DA1	Dual	185	4.5	86	± 2
6060_DA2	Dual	185	6	90	± 2
6060_DA3	Dual	195	6	92	± 2

The hardness results for the specimens subjected to the DA treatment are summarised in Table 18. The 6060_DA1 specimen exhibited the lowest hardness value, 86 HV, while the 6060_DA2 sample recorded 90 HV. In contrast, the highest hardness was achieved by the 6060_DA3 sample, with 92 HV. This value is noteworthy as it is equivalent to the peak hardness obtained under conventional ageing conditions. This behaviour indicates that, in dual ageing, an increase in both the final temperature and the total ageing time resulted in an increase in the hardness of the material. While the effect of ageing time is consistent with that observed in traditional processes, the influence of ageing temperature diverges, as lower temperatures are typically associated with maximising mechanical properties in conventional ageing [20].

This can be explained by using an intermediate temperature lower than the temperature of the conventional ageing treatments, such as 150 °C, which promotes a fine and dispersed nucleation of GP zones and β'' precipitates, thereby enhancing the material's maximum hardening potential. Subsequently, when a higher final ageing temperature is applied, these precipitates grow and develop while retaining their fine dispersion, which is an advantage compared to only using a single higher temperature. As a result, peak hardening can be achieved in significantly shorter times due to the combined effects of these two temperatures [43,44].

Regarding the final ageing temperature, studies show that, as in conventional ageing treatments, higher temperatures lead to peak hardening at shorter ageing times. This suggests that the 6060_DA2 specimen, aged at 185 °C, may not have yet reached peak hardening and would require a longer treatment time to achieve values similar to those obtained with specimen 6060_DA3, aged at 195 °C [20].

Therefore, DA has proven to be an effective strategy for achieving the peak of mechanical properties in considerably shorter processing times. This finding has significant implications for industrial efficiency and productivity, since the hardness peak is reached in approximately half the time required compared to a conventional ageing process.

Given the impossibility of manufacturing profiles under conventional ageing conditions, corresponding to peak hardness, the strength test of the ladder produced with the 6060_DA3 condition evaluated the mechanical performance at the maximum strength condition.

For a more in-depth analysis of the mechanisms underlying this hardening and strength gain, the hardness results were correlated with a microstructural analysis of the most representative specimens from the study.

4.3.2. Microstructural Analysis

Microstructural analysis of samples 6060_S, 6060_12h, and 6060_DA3 was conducted using two observation techniques: OM and SEM/EDS.

The primary objective of this analysis was to identify any differences or characteristics in the microstructures obtained with different ageing parameters, specifically in terms of grain size and chemical composition, quantity, dispersion, and morphology of the cooling and SHT precipitates. The need to understand if the ageing parameters have any influence on these points justifies the use of these analyses. Furthermore, the 6060_S specimen served as a control to provide a comparative baseline for the microstructure of the aged specimens.

The initial phase of this analysis involved OM, with the resulting images presented in Figures 25 to 29. This includes the 6060_DA1 and 6060_DA2 results, as it also facilitated the assessment of any effects of DA parameters on the material's microstructure.

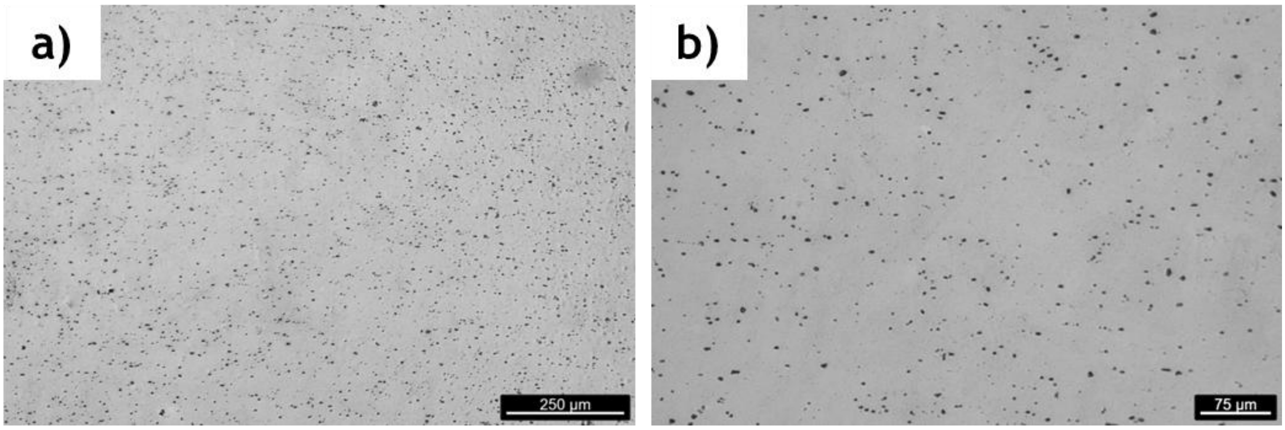

Figure 25: Microstructure of 6060 AA as-solubilised a) low magnification and b) high magnification.

The microstructural examination of the 6060_S specimen revealed an Al matrix with a dispersion of precipitates. According to the alloy's chemical composition, these precipitates are most likely intermetallic particles composed of Al, Fe, and Si, with a potential inclusion of Mn. The precipitates display a rounded morphology, characteristic of this condition after SHT [48].

A significant challenge in this analysis was the inability to distinctly delineate the grain boundaries via etching, as the process consistently resulted in over-etching of the precipitates. If the over-etching procedure was applied, the analysis of the morphology of these precipitates would be more difficult, which could compromise the study of the effectiveness of the SHT process.

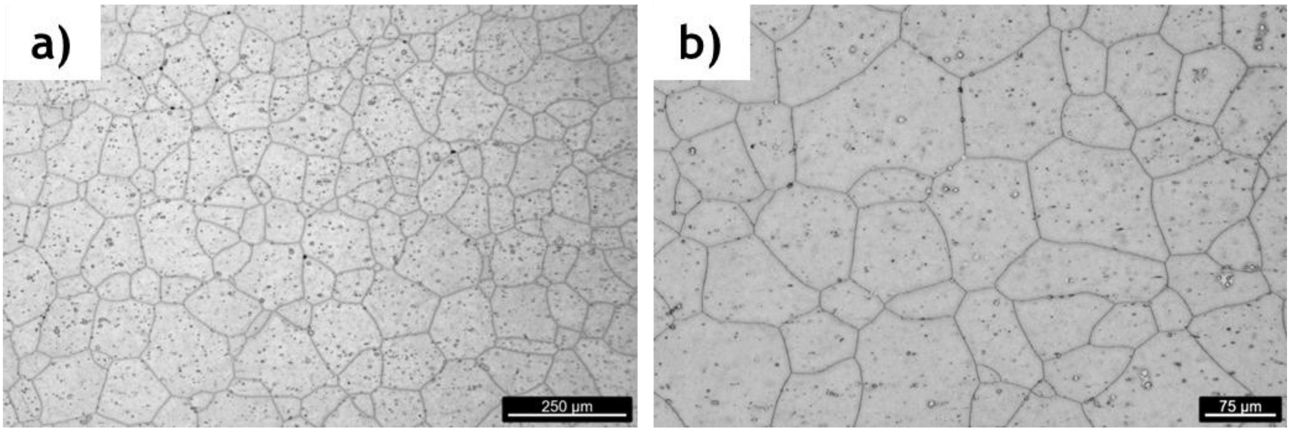

Figure 26: Microstructure of 6060 AA after ageing for 12 hours at 175 ºC a) low magnification and b) high magnification.

Regarding the 6060_12h specimen, corresponding to the identified peak hardness condition, the microstructure showed that the grain boundaries were clearly distinguishable. A significant variability in grain size was observed within this microstructure, with certain regions containing markedly smaller grains. The visible precipitates are distributed along the grain boundaries and within the grains, generally exhibiting a rounded and relatively uniform morphology, as confirmed by the SEM images (Figure 32). As discussed before in this document (section 4.1), the very fine dimensions strengthening precipitates cannot be directly identified in these images. Consequently, the visible precipitates are most likely intermetallic particles composed of Al, Fe, and Si that remained in the microstructure following SHT and ageing, as in the previous specimens analysed in section 4.1. These particles may serve as preferential nucleation sites for the strengthening precipitates during ageing, thereby contributing to the material's hardening process [48,50].

The comparison and analysis of the microstructures of the specimens subjected to DA, as shown in Figures 27 to 29, indicate that they exhibit very similar characteristics. Still, their grain sizes present slight differences between conditions. Examining the OM images of multiple regions within the same specimen has revealed that the grain size distribution seems to be notably heterogeneous, with some areas containing smaller grains, as can be verified in any of these three Figures. This observation suggests that a quantitative analysis across multiple fields would be warranted to attain a more comprehensive understanding of the potential influence of total ageing duration and final ageing temperature on grain growth. This would be even more important to allow a comparison between the conventional ageing and the DA influence on this microstructural characteristic, on the specimens that achieved the same peak hardness value (6060_12h and 6060_DA3).

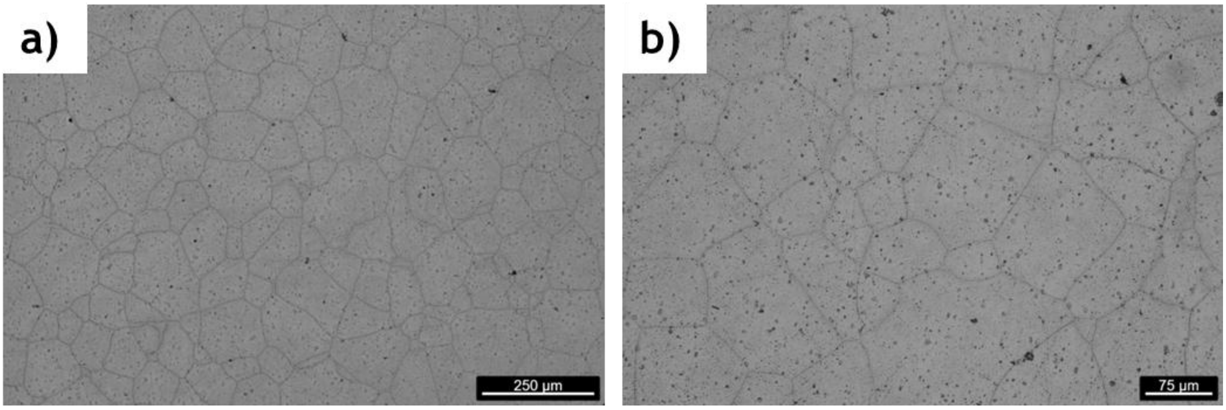

Figure 27: Microstructure of 6060 AA with DA at 185 ºC for 4.5 hours a) low magnification and b) high magnification.

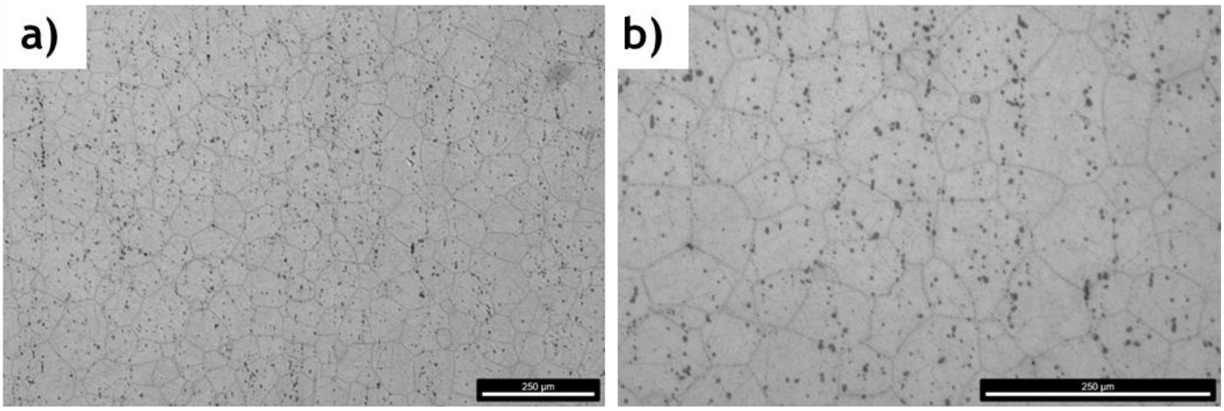

Figure 28: Microstructure of 6060 AA with DA at 185 ºC for 6 hours a) low magnification and b) high magnification.

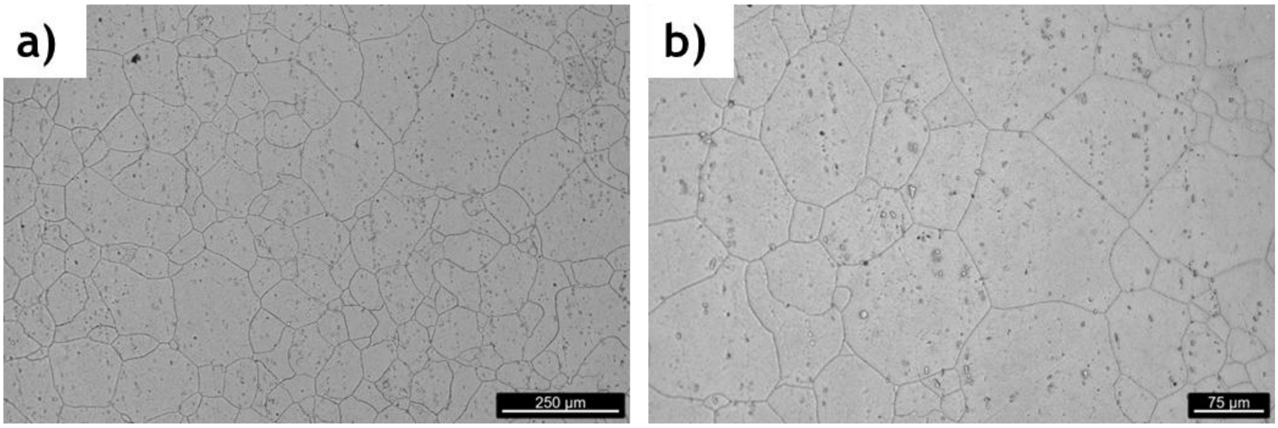

Figure 29: Microstructure of 6060 AA with DA at 195 ºC for 6 hours a) low magnification and b) high magnification.

Notwithstanding, the literature does not report a direct effect of ageing parameters on grain size, implying that these parameters influence grain size only indirectly [51]. This occurs because precipitation is ultimately correlated with grain size, as fine and well-dispersed precipitates assist in maintaining a more refined grain structure by acting as obstacles to grain boundary movement [52]. Based on that, prolonged ageing times or higher ageing temperatures can lead to overageing, where the precipitates coarsen and lose their effectiveness in retarding grain growth [51,53]. For this reason, the quantitative analysis of grain size through these OM images can represent a very useful information to be compared with a TEM analysis, in order to understand the relation between the hardening precipitates' size and dispersion with its control of grain size.

Microstructural analysis was further enhanced through SEM imaging, with particular focus on the 6060_S, 6060_12h, and 6060_DA3 samples, which are the most pertinent for examination, given that they represent the as-solutionised and as-peak conditions, respectively. The SEM and EDS analysis involved images at three different magnifications, as well as an examination of the chemical composition of both the matrix and the present precipitates. Figure 30 demonstrates the microstructure of the 6060_S specimen, where a matrix with rounded and uniform precipitates can be observed, thereby corroborating the assumptions derived from OM images.

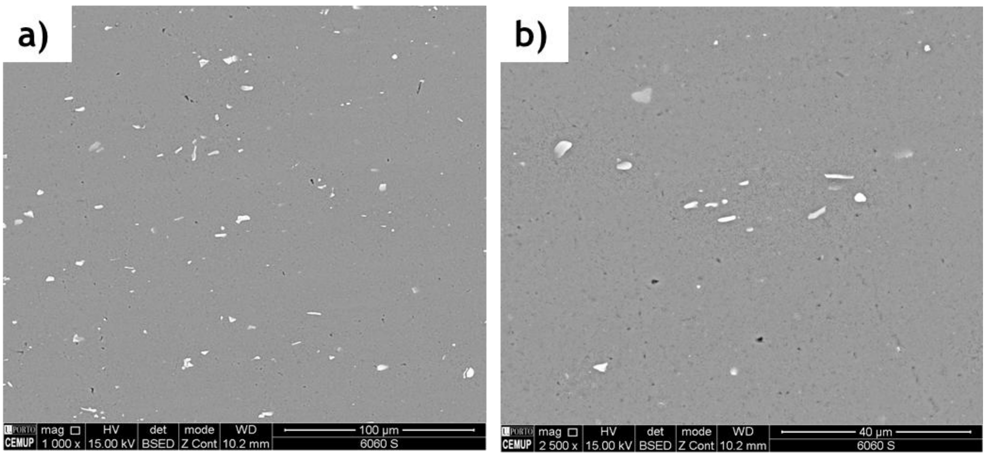

Figure 30: SEM images of the microstructure of 6060 AA as-solubilised a) low magnification and b) high magnification.

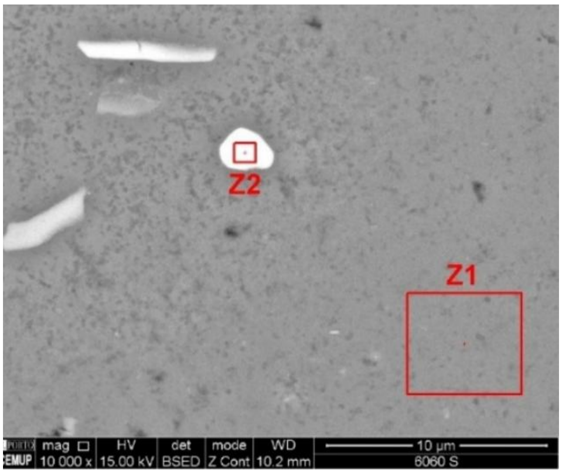

Figure 31: Identification of the zones of EDS analysis on the 6060_S specimen.

Table 19. Results of the EDS analysis on the 6060_S specimen.

ELEMENT	Wt%	
	Z1	Z2
Al	94.16	63.00
Fe	-	26.52
Mg	1.01	-
Mn	1.54	3.14
O	2.76	1.32
Si	0.52	6.02

The EDS analysis, as presented in Table 19, indicates that the observed precipitates are AlFeMnSi, exhibiting higher concentrations than in the matrix. These results align with expectations, given that these are the typical precipitates found in the as-solubilised condition structure of the 6060 AA [48]. Focusing the analysis on the specimens that underwent ageing and reached peak under different treatment conditions, Figure 32 presents the SEM microstructure of the 6060_12h and 6060_DA3 samples.

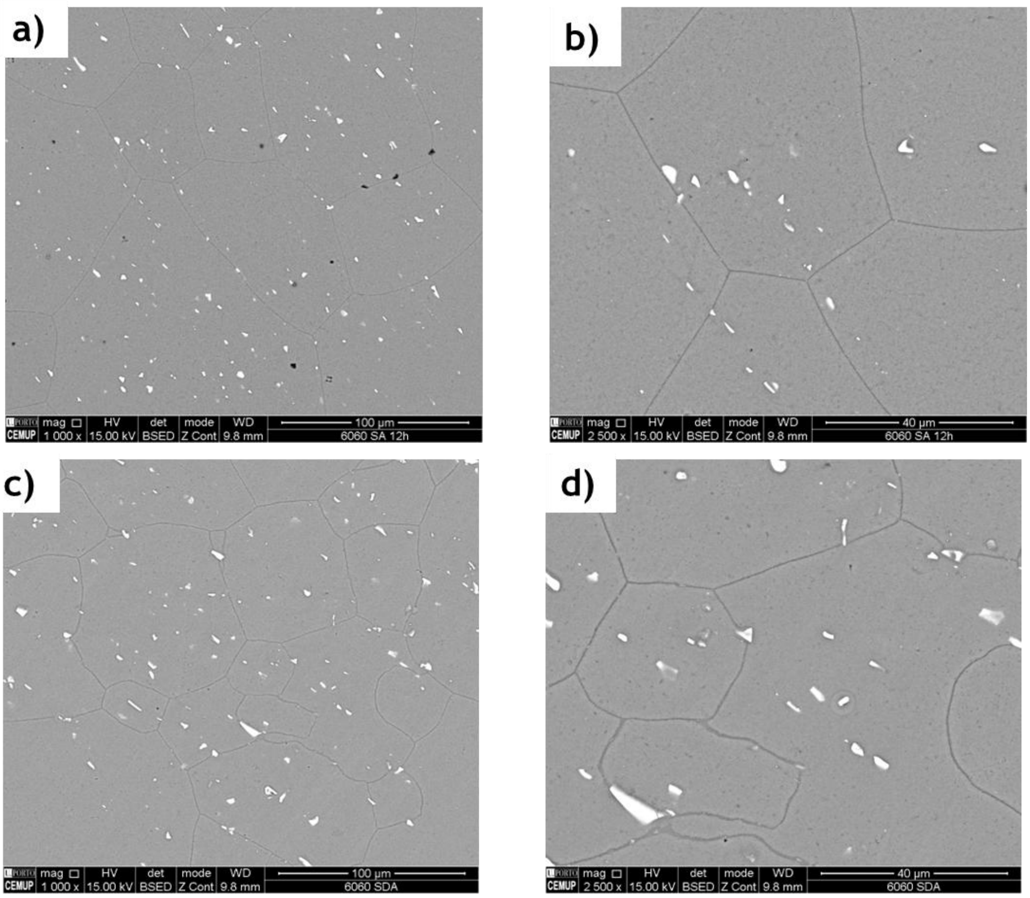

Figure 32: SEM images of the microstructure of a) 6060_12h specimen b) with a higher magnification c) 6060_DA3 specimen d) with a higher magnification.

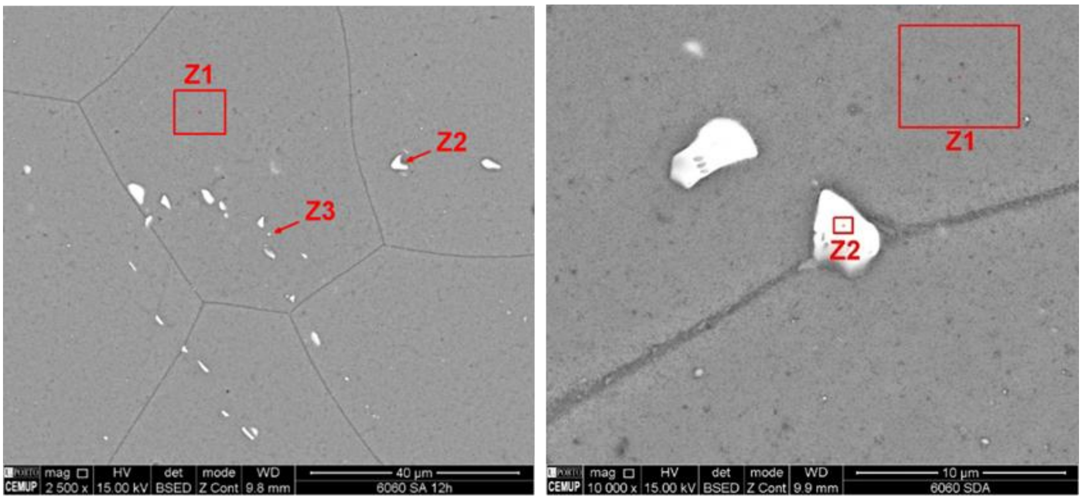

Figure 33: Identification of the zones of EDS analysis on the a) 6060_12h specimen b) 6060_DA3 specimen.

Table 20: Results of the EDS analysis on the 6060_12h and 6060_DA3 specimens.

ELEMENT	Wt %				
	6060_12H			6060_DA3	
	Z1	Z2	Z3	Z1	Z2
Al	94.41	72.62	84.48	93.99	68.93
Fe	-	19.82	9.12	-	21.33
Mg	0.94	-	-	1.21	0.52
Mn	1.52	1.53	1.90	1.53	1.57
O	2.54	1.16	2.41	2.79	1.79
SI	0.59	4.88	2.09	0.48	5.86

Analysis of the microstructures reveals that both specimens demonstrate a high density of precipitates distributed throughout the matrix. Both microstructures seem to present particles of similar size. However, a quantitative analysis of the particle size should also be conducted, based on these SEM images, since a bigger size of these particles can be attributed to the application of a higher ageing temperature. This occurs because, at higher temperatures, diffusion is accelerated, which promotes the coarsening of these particles and can influence the final properties of the alloy [54,55].

In both instances, the precipitates are primarily aligned in a particular direction, which is attributable to the extrusion process used during profile production, which induces this alignment. As observed in the OM images, the precipitates are present at the grain boundaries as well as within the grains, with no evident preferential localisation.

By analysing the chemical composition of the matrices as precipitates in these specimens, presented in Table 20, it was possible to infer that all identified precipitates correspond to solidification precipitates, composed of AlFeMnSi. This is also verified in region Z3, which contains smaller precipitates that could potentially be of the Mg-Si type.

This SEM analysis revealed that it is essential to understand the influence of specific heat treatment parameters on the size and chemical composition of the solidification and SHT precipitates, which can influence the final mechanical properties of the alloy.

Since neither of these analyses allows for the observation and analysis of the strengthening precipitates, which are composed of Mg and Si, a TEM analysis should also be conducted to understand how the ageing parameters influence their size, morphology, and stoichiometry. This information could also be connected to the results from the quantitative analysis of grain size, provided by the OM analysis, as mentioned above, to verify the influence of the precipitates' properties on the grain size and on the final mechanical properties. The importance of TEM analysis was already emphasised by several previous studies [39,48] to accurately identify these types of precipitates and evaluate their coherence with the matrix and morphology. Therefore, the utilisation of TEM would be highly advantageous for the analysis of the samples in this investigation, facilitating a more comprehensive understanding of the hardening mechanisms and the variations attributable to differences in heat treatment parameters.

XRD analysis has also been mentioned in earlier studies [56,57] as a solution to verify the presence of the hardening precipitates and their stoichiometry. However, it faces certain challenges, mainly due to the low phase fraction of these precipitates. This often prevents the detection of a distinct peak, making it difficult to identify their stoichiometry or even verify their presence.

In summary, these microstructural analyses provided further insight into the influence of ageing parameters on grain size and the final mechanical properties of the material, through changes in the size, coherence, and stoichiometry of hardening precipitates. Additionally, it was observed that solidification and SHT precipitates remain within the microstructure following the ageing process, with variations in their size and chemical composition, serving as preferential nucleation sites for hardening particles. It was also shown that for a better correlation between the ageing parameters and the final mechanical properties, quantitative grain size and TEM analyses should be conducted to establish a relationship between the grain size and the characteristics of the precipitates.

4.4. Ladder's Mechanical Performance Analysis

The mechanical performance of the produced ladders was evaluated through a vertical force test. This assessment was conducted across three dual ageing conditions and on 6061 AA in its as-received condition, for both profiles – 58 mm and 60 mm. Table 21 shows the results of this analysis.

Table 21: Results of the ladders strength tests.

LADDER	MAXIMUM SUPPORTED LOAD (N)	
	58 mm	60 mm
6060_DA1	2300	2600
6060_DA2	2400	-
6060_DA3	2400	2500
6061_AR	APPROVED	2650

Based on the results presented, it can be observed that, in the case of 6060 AA, the 60 mm profile consistently outperformed the 58 mm profile when tested under identical conditions. The variation in load capacity was consistent with the variation in sample hardness, increasing from condition 6060_DA1 (185 ºC, 4.5 h) to 6060_DA2 (185 ºC, 6 h) and subsequently to 6060_DA3 (195 ºC, 6 h). However, the ladder constructed with the 6060_DA1 60 mm profile exhibited the highest value among all, deviating from this general trend.

It was also observed that the peak hardening condition was insufficient in terms of strength to approve the ladder in the test, with the 60 mm profile falling short by 2000 N. Based on this, and on the conclusion that the 6060 AA, even at the peak strength, would not be sufficient to pass the test with these profiles, the alternative of using the 6061 AA in the as-received condition was investigated.

This alloy, which demonstrated superior hardness values, was successfully approved for the 58 mm profile, effectively withstanding a load of 2700 N for one minute, as mandated by the corresponding standard. However, the 60 mm profile unexpectedly failed the test, succumbing at a maximum load of 2650 N. It was essential to identify the factors influencing this behaviour to elucidate this discrepancy. The wall thickness is a crucial parameter in the control and inspection of profiles subjected to performance evaluations. Upon examination, it was determined that one of the side walls, at the failure location, had a thickness of 1.12 mm, contrary to the 1.3 mm specified in the technical drawing. Conversely, the opposite wall measured approximately 1.5 mm. It is most probable that this variation was caused by misalignment of the extrusion dies, resulting in a thinner wall section that was not only significantly offset from the intended geometry but also below the minimum thickness requirement specified by the standard (1.2 mm).

An additional significant aspect pertains to the testing procedure itself. The load was consistently applied manually by lowering a box containing the required load onto the step, as depicted in Figure 34. Nevertheless, due to the manual and inherently unstable nature of this method, considerable variability was observed across tests, particularly concerning the rate of load application, the placement of the load on the step where it was fixed, and the movement of the load. In certain instances, the load may be deposited more abruptly or unevenly, resulting in a more pronounced deformation of the material and affecting the failure threshold. To ensure the attainment of consistent and reliable results for each ladder, as well as for condition and profile testing, the procedure must ensure a continuous and uniform rate of load application, thereby maximising the reproducibility of the test.

In summary, the 6060 AA did not allow the ladders to fulfil the criteria for professional use. This objective was solely accomplished with 6061 AA, within the 58 mm profile.

Figure 34: Ladders Strenght Test setup.

Although 6061 AA is a more expensive material, choosing a 58 mm profile instead of a 60 mm one reduces the amount of raw material needed, creating a trade-off between these two factors. Balancing the profile geometry with alloy selection allows the company to test different scenarios and find the most efficient solution, not only in terms of performance but also from a commercial and economic perspective.

4.5. Raw material control and inspection: measures

The results of all the analyses performed in this study underscore the need for the company to establish and implement a comprehensive control and inspection plan for raw materials. Given that all Al processing is carried out externally, the requirement for rigorous monitoring of their properties assumes even greater importance. In line with the evaluations conducted in this research, the chemical compositions reported by suppliers must be systematically verified, with particular emphasis on the critical elements, namely Mg, Si and Fe. Since the company is already equipped with the necessary analytical instruments, this verification process can be facilitated and should be performed regularly, thereby reinforcing supplier accountability.

Furthermore, the dimensional characteristics of the profiles should be subjected to systematic inspection, with sampling protocols established for each bath. This approach enhances the ability to detect nonconforming products before they are introduced into production, thereby preventing the subsequent generation of scrap. Among the dimensional parameters, wall thickness constitutes the most critical aspect requiring control.

In addition to dimensional verification, the hardening state of the profiles must also be assessed, particularly through hardness testing. Currently, the company uses a Webster hardness tester, which exhibits an excessively high associated margin. The adoption of Brinell or Vickers hardness measurements would enable greater precision, especially considering that variations among conditions are relatively short.

By maintaining control over chemical composition, dimensional accuracy and hardening condition, the company will be able to reduce the portion of nonconforming products and, consequently, lower the scrap rate associated with these products.

5. CONCLUSIONS

5.1. Conclusions

This dissertation presents a methodology for the characterisation of AA and the optimisation of the entire production process of a product. Initially, two aluminium alloys, 6060 and 6061, were characterised in their as-received conditions. Subsequently, an analysis of the ladder production process was conducted to understand its impact on product failure, including an investigation into the underlying failure mechanisms. Finally, the heat treatment process for the 6060 AA was optimised to enhance its mechanical properties and overall performance. Ladder strength tests were performed following these stages to synthesise the research findings.

After this entire process, and based on the results presented earlier in Chapter 4, the following conclusions can be drawn:

1. The analysis of the chemical composition upon receipt of raw materials is an essential aspect. Deviations may occur between the supplier's certificate and the actual composition. Specifically, for Mg and Si, a variation in their ratio can impede the alloy from achieving optimal hardening, thereby resulting in the formation of alternative precipitates.
2. The 6061 AA in its as-received condition displayed superior mechanical properties compared to the 6060 AA under identical conditions, with the exception of elongation. For the 6060 AA, the measured hardness values were 88 HV10 and 82 HB 2.5/31.25, alongside a yield strength of 243 MPa, a tensile strength of 263 MPa, and an elongation of 12%. Conversely, the 6061 AA exhibited hardness values of 100 HV10 and 93 HB 2.5/31.25, with tensile properties including a yield strength of 269 MPa, a tensile strength of 288 MPa, and an elongation of 10%.
3. The ladder production process does not negatively impact the final product's performance, since there is no increasing work hardening as the process progresses, which was a crucial aspect to verify, particularly in the first three stages. Moreover, no cracks larger than 0.150 mm were observed during the CT failure analysis, indicating that failure occurs solely through plastic deformation mechanisms.
4. The maximum hardening condition for the 6060 AA is attained after 12 hours of ageing treatment at 175 ºC, achieving a hardness of 92 HV10. It is concluded that extended ageing durations may result in increased hardness values until the overaging phenomenon occurs. The MO and SEM analyses allowed for the observation of grain size and solidification, as well as SHT particles, in the specimens' microstructure. This can be used for quantitative analysis to determine the influence of the ageing parameters on these characteristics and on the final mechanical properties.
5. The implementation of DA treatments, incorporating an intermediate temperature step, facilitates the attainment of equivalent mechanical properties within a substantially reduced timeframe. In particular, the peak condition of the 6060 AA alloy, achieved through 12 hours of conventional ageing at 175 ºC, was replicated

by a dual ageing process with a final ageing temperature of 195 ºC and a total ageing duration of 6 hours. This duration is half that necessary for the standard treatment.

6. The 60 mm profile demonstrated superior performance in the ladder strength test relative to the 58 mm profiles on the 6060 AA, suggesting that the shape factor has an impact on the product's performance.
7. The 6060 AA in its optimised condition did not possess enough properties to pass the ladder's strength test. Approval was only granted with the use of the 6061 AA on the 58 mm profiles. It can also be concluded that the profile wall thickness is a vital factor to check upon receipt of raw materials, as a thickness less than the design specification can lead to product failure.
8. The way the test is performed at the company introduces a high level of error since the load is applied manually and unstably, without a fixed or reproducible rate. This can cause products with identical processing to produce different results, complicating the entire optimisation project.

5.2. Future work perspectives

Although product approval has been secured, additional inquiries for ongoing research and supplementary tests remain pertinent.

As mentioned earlier (chapter 4), a quantitative analysis of grain size and precipitate size should be performed to establish a more in-depth correlation between the ageing parameters and the mechanical properties of the material, based on the points mentioned before. For the same reason, a TEM analysis should also be conducted to allow the observation and analysis of the hardening precipitates.

To ensure comparability of the analysis results for each condition across various alloys, conducting tensile tests would be highly advantageous. Such tests would facilitate establishing a correlation between hardness and tensile strength, thereby enabling future extrapolation of this mechanical property through hardness testing alone.

Furthermore, investigating the 6060 alloy in its maximum strengthening condition by employing a greater profile wall thickness could prove advantageous. This approach may provide an improved balance between the alloy employed and the quantity of raw material required, especially considering that raw material cost constitutes the largest proportion of the company’s expenses.

REFERENCES

[1] Ferral – José Luís & Ca. Lda., "The company," Ferral, Jun. 12, 2025. [Online]. Available: https://ferraljl.com/pt/a-empresa/. [Accessed: June 22, 2025].

[2] Ferral – José Luís & Ca. Lda., "Quality and Certification," Ferral, Dec. 4, 2024. [Online]. Available: https://ferraljl.com/pt/qualidade/. [Accessed: June 22, 2025]

[3] E. Bossi, "Commodity market risk: derivates hedging for the aluminium market," M.Sc. thesis, Econ., Finance & Sustainability, University of Ca' Foscari Venezia, Venice, Italy, 2023. [Online]. Available: https://unitesi.unive.it/retrieve/bc734636-4913-4fe5-adfa-a14aff20a85c/888309-1274779.pdf

[4] K. Hosová, J. Kubásek, M. Straková, and D. Nečas, "Material Properties of Firefighter Ladder Composed from AA6063 and Few Other Aluminium-Based Alloys, *Manufacturing Technology*, vol. 20, no. 6, pp. 748–754, Dec. 2020, doi: 10.21062/mft.2020.101.

[5] M. T. Alam and A. Ansari, "Review on Aluminium and its Alloys for Automotive Applications," *International Journal of Advanced Technology In Engineering and Science*, vol. 5, pp. 278–294, May 2017.

[6] J. Hirsch, "Recent development in aluminium for automotive applications," *Transactions of Nonferrous Metals Society of China*, vol. 24, no. 7, pp. 1995–2002, Jul. 2014, doi: 10.1016/S1003-6326(14)63305-7.

[7] S. Capuzzi and G. Timelli, "Preparation and Melting of Scrap in Aluminium Recycling: A Review," *Metals*, vol. 8, no. 4, p. 249, Apr. 2018, doi: 10.3390/met8040249.

[8] K. Georgitzikis, L. Mancini, E. D'Elia, and B. Vidal-Legaz, *Sustainability aspects of Bauxite and Aluminium*. EUR, no. 30760. Publications Office of the European Union, Luxembourg, 2021. doi: 10.2760/702356.

[9] D. Ashkenazi, "How aluminium changed the world: A mettalurgical revolution through tecnological and cultural perspectives," *Technological Forecasting and Social Change*, vol. 143, pp. 101–113, Jun. 2019, doi: 10.1016/j.techfore.2019.03.011.

[10] J. I. Rajan, "Development of ultrafine grained A356 aluminium alloy by severe plastic deformation and studies on its deformation behaviour and machinability," Ph.D. thesis, Indian Institute of Technology Bhilai, Bhilai, India, Mar. 2017. [ONLINE]. Available: https://www.researchgate.net/publication/324112090_Development_Of_Ultrafine_Grained_A356_Aluminium_Alloy_By_Severe_Plastic_Deformation_And_Studies_On_Its_Deformation_Behaviour_And_Machinability.

[11] F. M. Mazzolani, "Competing issues for aluminium alloys in structural applications," *Progress Structural Eng Maths*, vol. 6, n.º 4, pp. 185–196, out. 2004, doi: 10.1002/pse.178.

[12] N. E. Prasad and R. J. H. Wanhill, Eds., Aerospace Materials and Material Technologies - Volume 1: Aerospace Materials. Singapore: Springer, Singapore, 2017. doi: 10.1007/978-981-10-2134-3.

[13] L. Sweet, S. M. Zhu, S. X. Gao, J. A. Taylor, and M. A. Easton, “The Effect of Iron Content on the Iron-Containing Intermetallic Phases in a Cast 6060 Aluminium Alloy,” *Metall Mater Trans A*, vol. 42, no. 7, pp. 1737–1749, Jul. 2011, doi: 10.1007/s11661-010-0595-6.

[14] M. S. Silva, C. Barbosa, O. Acselrad, and L. C. Pereira, “Effect of Chemical Composition Variation on Microstructure and Mechanical Properties of a 6060 Aluminum Alloy,” *Journal of Materials Engineering and Performance*, vol. 13, no. 2, pp. 129–134, Apr. 2004, doi: 10.1361/10599490418307.

[15] F. Ozturk, A. Sisman, S. Toros, S. Kilic, and R. C. Picu, “Influence of aging temperature on mechanical properties of 6061 aluminium alloy,” *Materials & Design*, vol. 31, no. 2, pp. 972–975, Feb. 2010, doi: 10.1016/j.matdes.2009.08.017.

[16] C. Menapace, F. Bernard, M. Lusa, G. Ischia, e G. Straffelini, “Effect of dual-rate ageing treatment on the tensile properties of a commercial 6060 Al alloy,” *Materials Science and Engineering: A*, vol. 819, p. 141468, Jul. 2021, doi: 10.1016/j.msea.2021.141468.

[17] Ansys Inc., “Aluminum 6060,” Granta Edupack 2024 R2, [Software]. Cambridge, UK: Ansys, 2025.

[18] Ansys Inc., “Aluminum 6063,” Granta Edupack 2024 R2, [Software]. Cambridge, UK: Ansys, 2025.

[19] S. Nandy, Md. A. Bakkar, and D. Das, “Influence of Ageing on Mechanical Properties of 6063 Al Alloy,” *Materials Today: Proceedings*, vol. 2, no. 4–5, pp. 1234–1242, 2015, doi: 10.1016/j.matpr.2015.07.037.

[20] A. Munitz, C. Cotler, and M. Talianker, “Ageing impact on mechanical properties and microstructure of Al-6063,” J. Mater. Sci. vol. 35, no. 11, pp. 2529-2538, May 2000. [Online]. Available: https://doi.org/10.1023/A:1004742407600.

[21] Krishna Pal Singh, “Influence of Heat Treatment on the Mechanical Properties of Aluminium Alloys (6xxx Series): A Literature Review,” *IJERT*, vol. 6, no. 3, Mar. 2017, doi: 10.17577/ijertv6is030301.

[22] Ansys Inc., “Aluminum 6061,” Granta Edupack 2024 R2, [Software]. Cambridge, UK: Ansys, 2025.

[23] H. Demir and S. Gündüz, “The effects of aging on machinability of 6061 aluminium alloy,” *Materials & Design*, vol. 30, no. 5, pp. 1480–1483, May 2009, doi: 10.1016/j.matdes.2008.08.007.

[24] C. María Abreu Fernández, R. A. Rey, M. Julia Cristóbal Ortega, D. Verdera, and C. L. Vidal, “Friction stir processing strategies to develop a surface composite layer on AA6061_T6,” *Materials and Manufacturing Processes*, vol. 33, no. 10, pp. 1133-1140, Jul. 2018, doi: 10.1080/10426914.2017.1415447.

[25] Lorraine F. Francis, “Chapter 4 – Solid Processes,” Materials Processing, Academic Press, pp. 251-342, 2016. [Online]. Available: https://doi.org/10.1016/B978-0-12-385132-1.00004-5.

[26] Industrial Quick Search, “Process, properties and benefits of extruded aluminum,” IQS Directory, [Online]. Available: https://www.iqsdirectory.com/articles/aluminum-extrusion/extruded-aluminum.html#overview-of-extruded-aluminum.

[27] M. P. Groover, *Fundamentals of Modern Manufacturing: Materials, Processes and Systems*, 4th ed. Hoboken, NJ, USA: Wiley, 2010. ISBN 978-0470467008.

[28] X. Kuangdi, Ed., *The ECPH Encyclopedia of Mining and Metallurgy*. Singapore: Springer Nature Singapore, 2024. doi: 10.1007/978-981-99-2086-0.

[29] N. Berndt, P. Frint, M. Böhme, and M. F.-X. Wagner, “Microstructure and mechanical properties of an AA6060 aluminum alloy after cold and warm extrusion,” *Materials Science and Engineering: A*, vol. 707, pp. 717–724, nov. 2017, doi: 10.1016/j.msea.2017.09.040.

[30] A. S. Chahare, “Optimization of Aluminium Extrusion Process using Taguchi Method,” *IOSR JMCE*, vol. 17, no. 01, pp. 61–65, Mar. 2017, doi: 10.9790/1684-17010016165.

[31] N. C. W. Kuijpers, W. H. Kool, P. T. G. Koenis, K. E. Nilsen, I. Todd, and S. Van Der Zwaag, “Assessment of different techniques for quantification of α-Al(FeMn)Si and ß-AlFeSi intermetallics in AA 6xxx alloys,” *Materials Characterization*, vol. 49, no. 5, pp. 409–420, Dez. 2002, doi: 10.1016/S1044-5803(03)00036-6.

[32] M. Baruah e A. Borah, “Processing and Precipitation Strengthening of 6xxx Series Aluminium Alloys: a Review,” *Int. J. Mater. Sci.*, vol. 1, no. 1, pp. 40–48, Jan. 2020, doi: 10.22271/27078221.2020.v1.i1a.10.

[33] W. Kuijpers, F. Vermolen, K. Vuik, and S. Zwaag, “A Model of the ß-AlFeSi to α-Al(FeMn)Si Transformation in Al-Mg-Si Alloys,” *Mater. Trans.*, vol. 44, no. 7, pp. 1448–1456, 2003, doi: 10.2320/matertrans.44.1448.

[34] N. Bayat, T. Carlberg, and M. Cieslar, “In-situ study of phase transformations during homogenization of 6060 and 6063 Al alloys,” *Journal of Physics and Chemistry of Solids*, vol. 130, pp. 165–171, Jul. 2019, doi: 10.1016/j.jpcs.2018.11.013.

[35] S. O. Adeosun, S. A. Balogun, O. I. Sekunowo, and M. A. Usman, “Effects of Heat Treatment on Strength and Ductility of Rolled and Forged Aluminum 6063 Alloy,” *JMMCE*, vol. 09, no. 08, pp. 763–773, 2010, doi: 10.4236/jmmce.2010.98054.

[36] I. De Silva, A. Perera, N. Kodikara and A. De Silva, “Improving the mechanical properties of aluminum 6063 structural items by varying the chemical composition,” in Proceedings of the EFCECM 2014, Manado, Indonesia, 2014. [ONLINE]. Available: https://repo.unsrat.ac.id/1701/1/EFCECM%202014%20Proceeding%20eBook%20updated.pdf#page=249.

[37] A. Ahmad, N. Afzal, and M. Rafique, “Structural and mechanical response of artificially aged aluminum alloy 6061,” *Strength Mater*, vol. 53, no. 3, pp. 502–510, May. 2021, doi: 10.1007/s11223-021-00311-0.

[38] A. Poznak, D. Freiberg, e P. Sanders, “Chapter 10 – Automotive Wrought Aluminium Alloys,” in *Fundamentals of Aluminium Metallurgy*, Elsevier, 2018, pp. 333–386. doi: 10.1016/B978-0-08-102063-0.00010-2.

[39] C. D. Marioara, H. Nordmark, S. J. Andersen, and R. Holmestad, “Post-β” phases and their influence on microstructure and hardness in 6xxx Al-Mg-Si alloys,” *J Mater Sci*, vol. 41, no. 2, pp. 471–478, Jan. 2006, doi: 10.1007/s10853-005-2470-1.

[40] P. Osuch, M. Walkowicz, T. Knych, and S. Dymek, “Impact of Direct Ageing Procedure on the Age Hardening Response of Al-Mg-Si 6101 alloy,” *Materials*, vol. 11, no. 7, p. 1239, Jul. 2018, doi: 10.3390/ma11071239.

[41] R. Donovan, R. Fortune and R. Trout, “Elevated Temperature Effects on the Mechanical Properties of Age Hardened 6xxx Aluminum Alloy Extrusions,” M.Sc. thesis, Materials Engineering Department, California State University, 2015. [Online]. Available: https://www.researchgate.net/publication/304165452_Elevated_Temperature_Effects_on_the_Mechanical_Properties_of_Age_Hardened_6xxx_Series_Aluminum_Alloy_Extrusions

[42] H. He, L. Zhang, S. Li, X. Wu, H. Zhang, and L. Li, “Precipitation Stages and Reaction Kinetics of AlMgSi Alloys during the Artificial Aging Process Monitored by In-Situ Electrical Resistivity Measurement Method,” *Metals*, vol. 8, no. 1, p. 39, Jan. 2018, doi: 10.3390/met8010039.

[43] A. M. Niederer, “*Two-Step Artificial Ageing of 6xxx Aluminium Wrought Alloys,”* M.SC. Thesis, Technische Universität Wien. 2016. [Online]. Available: https://doi.org/10.34726/hss.2016.30582

[44] N. Berndt, P. Frint, and M. Wagner, “Influence of Extrusion Temperature on the Aging Behavior and Mechanical Properties of an AA6060 Aluminum Alloy,” *Metals*, vol. 8, no. 1, p. 51, Jan. 2018, doi: 10.3390/met8010051.

[45] W. D. Callister and D. G. Rethwisch, “Dislocations and Strengthening Mechanisms,” in Materials Science and Engineering: an Introduction, 10th ed. Hoboken, NJ, USA: Wiley, 2018, ch. 7, pp. 223-268.

[46] M. R. Akbarpour *et al.*, “Recent advances in processing, and mechanical, thermal and electrical properties of Cu-SiC metal matrix composites prepared by powder metallurgy,” *Progress in Materials Science*, vol. 140, p. 101191, Dez. 2023, doi: 10.1016/j.pmatsci.2023.101191.

[47] F. Meng, H. Huang, X. Yuan, X. Lin, Z. Cui, and X. Hu, “Segregation in squeeze casting 6061 aluminum alloy wheel spokes and its formation mechanism,” *China Foundry*, vol. 18, no. 1, pp. 45–51, Jan. 2021, doi: 10.1007/s41230-021-0079-x.

[48] J. S. Aristeidakis *et al.*, “Microstructural Evolution in a 6060 Extrudable Al-Alloy: Integrated Modeling and Experimental Validation,” *Materials*, vol. 17, no. 3, p. 545, Jan. 2024, doi: 10.3390/ma17030545.

[49] V. Bokyo, “Characterization of the structure and precipitation process in Al-Mg-Si and Al-Mg-Ge casting alloys,” Ph.D. dissertation, University of Science and Technology, Krakow, Poland, Jan. 2015. [Online]. Available: https://www.researchgate.net/publication/307929599_Characterization_of_the_structure_and_precipitation_process_in_Al-Mg-Si_and_Al-Mg-Ge_casting_alloys.

[50] P. Sarafoglou, J. Aristeidakis, M.-I. Tzini, and G. Haidemenopoulos, “Metallographic Index-Based Quantification of the Homogenization State in Extrudable Aluminum Alloys,” Metals, vol. 6, no. 5, p. 121, May 2016, doi: 10.3390/met6050121.

[51] K. Au and M. Hodgson, “Studies On Age Hardening For Improvement Of 6261 And 6060 Extruded Aluminium Alloys,” Int. J. Mod. Phys. B, vol.24, no. 15-16, pp. 2467-2475, 2010. [Online]. Available. https://doi.org/10.1142/S0217979210064757.

[52] I. Sevim, S. Sahin, H. Cug, E. Cevik, F. Hayat, and M. Karali, “Effect Of Aging Treatment On Surface Roughness, Mechanical Properties, And Fracture Behavior Of 6xxx And 7xxx Aluminum Alloys,” *Strength Mater*, vol. 46, no. 2, pp. 190–197, Mar. 2014, doi: 10.1007/s11223-014-9535-9.

[53] O. Adem, “Effects of artificial aging heat treatment on mechanical properties and corrosion behaviour of AA6XXX aluminium alloys,” *J. Chem. Eng. Mater. Sci.*, vol. 9, no. 2, pp. 17–23, Set. 2018, doi: 10.5897/JCEMS2018.0315.

[54] D. V. Quang, L.T.V. Anh, V. T. Huong, N. Q. Tuan, “Influences of ageing parameters on the microstructure and mechanical properties of extruded 6063 and 6005 alloys,” *VMOST*, vol. 66, no. 4, Dez. 2024, doi: 10.31276/VJSTE.2024.0020.

[55] F. Mao, *Investigation and Modelling of Precipitate Evolution in Age-Hardenable Al-Alloys During Artificial Ageing*, Ph.D. dissertation, RWTH Aachen, Germany, 2019. [Online]. Available: https://publications.rwth-aachen.de/record/766189/files/766189.pdf

[56] S. K. Panigrahi, R. Jayaganthan, and V. Pancholi, “Effect of plastic deformation conditions on microstructural characteristics and mechanical properties of Al 6063 alloy,” Materials & Design, vol. 30, no. 6, pp. 1894–1901, Jun. 2009, doi: 10.1016/j.matdes.2008.09.022.

[57] G. Mrówka-Nowotnik, J. Sieniawski, and M. Wierzbiñska, “Intermetallic phase particles in 6082 aluminium alloy,” *Archives of Materials Science and Engineering*, vol. 28, no. 2, pp 69-76, Jan. 2007.

APPENDIX A

6th DOCTORAL CONGRESS IN ENGINEERING

U.PORTO FEUP FACULDADE DE ENGENHARIA UNIVERSIDADE DO PORTO

30 JUN - 1 JUL | 2025

Enhancing the Structural Integrity of Aluminium Combination Ladders: the role of microstructure and mechanical performance on heat treatment optimisation

Ana Figueiredo[1,*], Regina Coelho[1], Luís Filipe Silva[2], Manuel F. Vieira[1,3], Elsa W. Sequeiros[1,3]

[1] DEMec/FEUP - Faculty of Engineering of the University of Porto, Rua Drº Roberto Frias s/n, Porto, Portugal.
[2] FERRAL – José Luís & Ca. Lda., Rua dos Sobrais 655, Zona Industrial Sul -apartado 70, Cortegaça Ovar, Portugal.
[3] LAETA/INEGI – Institute of Science and Innovation in Mechanical and Industrial Engineering, Rua Drº Roberto Frias 400, Porto, Portugal
* Presenting author email: up202005630@edu.fe.up.pt

INTRODUCTION | OBJECTIVES

Aluminium 6xxx series alloys are essential to the ladder industry due to their exceptional combination of mechanical strength, low weight, corrosion resistance, and manufacturability. Aluminium Alloys such as 6061, 6060 6063, and 6082 are specifically engineered to provide a high strength-to-weight ratio, making them ideal for constructing ladders that are both durable and portable [1]. The primary alloying elements in 6xxx series Aluminium Alloys are magnesium (Mg) and silicon (Si). These alloys derive their strength primarily from the formation of the intermetallic compound Mg_2Si, which precipitates during heat treatment. The strengthening mechanism, known as precipitation hardening, involves a solution treatment followed by artificial aging. This process enables controlled growth of the precipitates within an aluminium-rich matrix, significantly enhancing the mechanical properties of the alloy [2]. In order to enhance the mechanical properties of Aluminium Combination Ladders, an investigation was carried out under the scope of the Project "Projeto FEUP-FERRAL." where Heat Treatment Tests were conducted using various combinations of aging time and aging temperature.

MATERIALS & METHODS

STUDY MATERIAL: 606090 Aluminium Alloy

Chemical composition of 606090 Aluminium Alloy.

ELEMENT	Si	Fe	Cu	Mn	Mg	Cr	Zn	Pb	Al
ELEMENT FRACTION (%)	0.53	0.20	0.00	0.02	0.52	0.00	0.00	0.001	98.71

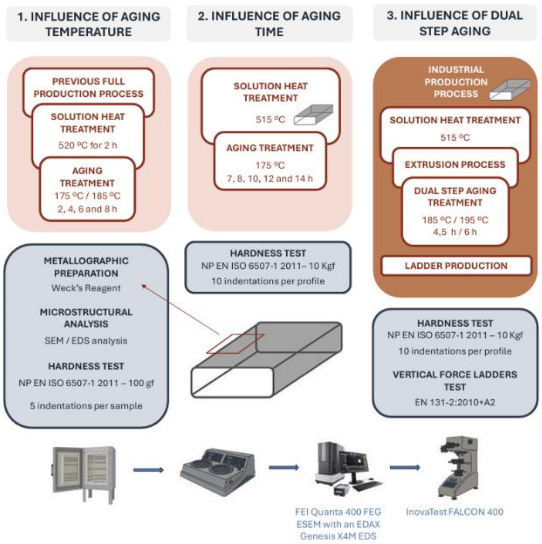

RESULTS & DISCUSSION

As shown in Figure 1, hardness increases with ageing time. Nevertheless, at prolonged aging durations, the hardness values at 185 °C decrease and fall below those observed at 175 °C. Since the peak aging time for this alloy at 175 °C was not reached, a new investigation was carried out where the entire extruded profiles were used without applying the industrial aging treatment, allowing for the evaluation of all aging durations. The corresponding results are shown in Figure 2, and it showed a slight increase in hardness with aging time; however, the variation was minimal, with only a 1 HV difference between conditions. This declares that a partial natural aging may have occurred, as the hardness value of the control profile is higher than that of the solution heat-treated (SHT) profile, which may explain the slight differences between the conditions.

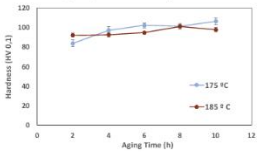

Figure 1. Effect of Aging Time on the Hardness of 606090 Aluminium Alloy Longitudinal Samples at Different Temperatures.

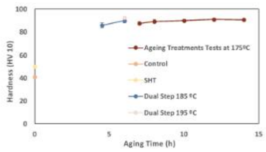

Figure 2. Effect of Aging Time on the Hardness of 606090 Aluminium Alloy profiles at Different Temperatures.

Table 2. Results of the Vertical Force Ladders Test.

PROFILE THICKNESS	Maximum weight (Kg) 185 ºC 4,5 h	185 ºC 6 h	195 ºC 6 h
< thickness	230	240	240
> thickness	260	NOT TESTED	250

As shown in Table 2, a better performance was obtained using:

- Higher profile thickness
- Longer aging time

ELEMENT	Wt (%) Z1 a)	Z1 b)	Z1 c)	Z2 a)	Z2 b)	Z2 c)	Z3 a)	Z3 b)	Z3 c)
Al	95.70	95.69	96.86	66.30	68.07	78.09	64.81	77.27	66.87
Fe	-	-	-	18.69	22.79	12.94	21.85	12.11	23.88
Mg	1.05	1.05	1.04	0.50	-	0.68	-	1.40	0.43
Mn	-	-	-	1.62	1.15	1.96	2.93	0.76	1.16
O	2.55	2.58	1.75	3.31	1.81	1.74	2.66	1.87	2.13
Si	0.70	0.67	0.34	9.58	6.17	4.59	7.75	6.59	5.53
TOTAL	100	100	100	100	100	100	100	100	100

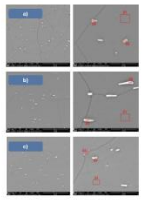

Figure 3. Images of the SEM/EDS analysis on dual step aging samples: a) 185 ºC – 4,5 h b) 185 ºC – 6 h c) 195 ºC - 6 h

The particles observed on Figure 3, exhibit a higher concentration of Fe and Si compared to the matrix, indicating that they are AlFeSi particles. These particles can contribute positively to enhancing mechanical properties by acting as preferential nucleation sites for Mg2Si precipitates during the aging treatment and, additionally, they improve microstructural uniformity and reduce residual stress concentrations [3, 4]. After aging, some of these particles may persist in the microstructure, depending on the aging parameters used [3].

CONCLUSION

- Higher aging times lead to increased hardness values, up to the point of overaging.
- Lower aging temperatures result in a higher hardness peak but require longer aging times.
- The Dual Step Aging Treatment allows to get the same hardness values with a shorter aging time.
- There were remaining AlFeSi particles on the microstructure after aging and to observe the Mg_2Si particles, another observation techniques are needed.

ACKNOWLEDGEMENTS

This research was supported by Project "Projeto FEUP-FERRAL".

U.PORTO FEUP FACULDADE DE ENGENHARIA UNIVERSIDADE DO PORTO

FERRAL®

APPENDIX B

A previous study was conducted using the 6060 AA. The material was solution heat treated at 520 °C for 2 hours and then aged at 175 °C and 185 °C for different times. This was performed to understand the influence of the ageing temperature on the material's hardness and mechanical properties.

The results are shown in Figure 1.

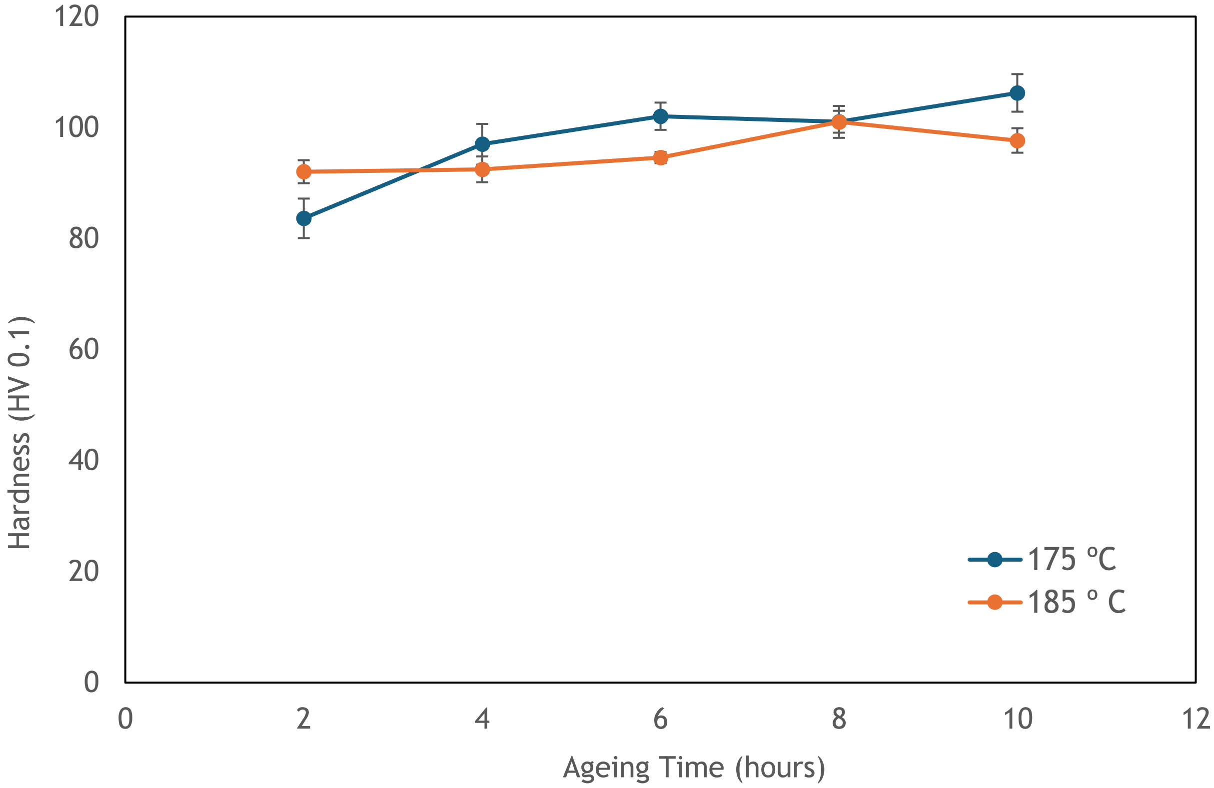

Figure 1: Influence of ageing time and temperature on the hardness of a 6060 AA.

The results showed that the 185 °C temperature reached the peak condition at 8 hours, while the 175 °C didn't reached that condition, but already achieve higher hardness values. As mentioned in the literature review (section 2), lower ageing temperatures allow to achieve higher peak hardness values but require longer ageing times. This was confirmed in this study and, for that reason, the 175 °C was the chosen temperature for the conventional ageing treatments of this study.